FLJ23538/clone 137308, 5′-GAG AGG GTT GGT TAG AGA TAC-3′ (forward) and 5′-TGA TTT TAG GTG ATA GTT TCC-3′ (reverse); integrin α7, 5′-AAG ACC GAC AGC AGT TCA AGG-3′ (forward) and 5′-GAC GAA ACC ACG AAA CCA CTA-3′ (reverse); *SLC20A1* (solute carrier family 20, member 1), 5′-TAT GTT TGG TTC TGC TGT GTC-3′ (forward) and 5′-GCT ATC TAT GCT GGT TTC CTC-3′ (reverse); *ENPP2* (ectonucleotide pyrophosphatase/phosphodiesterase-2), 5′-TTC TTT TGG TCT GTG TCA TC-3′ (forward) and 5′-TTC TTC TGT TGT TGG CAT AGT-3′ (reverse); *SEPP1* (selenoprotein P, plasma, 1), 5′-GGA ACA GAG AGC CAG GAC CA-3′ (forward) and 5′-CCT ATG CTG ACC CTT GTG CTT-3′ (reverse); stanniocalcin-1, 5′-AAG AAA GAA AGA GGG AAA AAG-3′ (forward) and 5′-AAC CAA ATC ACA AGG AAA GAA-3′ (reverse); *ETV5* (Ets variant gene-5), 5′-TTG TGT TGT GCC TGA GAG ACT-3′ (forward) and 5′-TCT ATG GGT TTG TGA TTT TTC-3′ (reverse); *NDRG1* (N-Myc downstream regulated gene-1), 5′-GCG GTG GCT GAG AAA ATG TAA-3′ (forward) and 5′-CAA GGT GAT GGG CGG CAG GTA-3′ (reverse); *ARHE* (Ras homolog gene family, member E), 5′-ACT TCG GGT TCT CCT TAC TAT-3′ (forward) and 5′-TTC TCA TCA CTT GGT CTA CAT-3′ (reverse); *HSTF2* (heat shock transcription factor-2), 5′-CAG AAC CAA CCC AAA GTA AGC-3′ (forward) and 5′-ACA GCA TCA ACA GGA AAA CA-3′ (reverse); *NTHL1* (Nth endonuclease III-like 1 (*E. coli*)), 5′-CAG CAG AAG CGA GGA AAA GC-3′ (forward) and 5′-CGC GCA GAG GGC TTG GTT GAG-3′ (reverse); *RGS16* (regulator of G-protein signaling-16), 5′-TGA GAG TCC TGC TGA AAT CCA-3′ (forward) and 5′-CCA ACA ATA ACA AAA ACA ATG-3′ (reverse); hexokinase-2, 5′-GAA CTG GTG GAA GGA GAA GAG-3′ (forward) and 5′-AGG GAA GAA GGA GAG AAA GAG-3′ (reverse); *LTA1* (L-type amino acid transporter subunit-1), 5′-TCG GGG TCT GGT GGA AAA ACA-3′ (forward) and 5′-AAC AAA GGA GGG AAG GGA AAA-3′ (reverse); *SLC1A3* (solute carrier family 1, member 3), 5′-TAT GTT TGG TTC TGC TGT GTG-3′ (forward) and 5′-GCT ATC TAT GCT GGT TTC CTC-3′ (reverse); and β-actin, 5′-CAG CAA GCA GGA GTA TGA CGA-3′ (forward) and 5′-GTG GAC TTG GGA GAG GAC TGG-3′ (reverse). The number of cycles was selected to allow linear amplification of the cDNA under study. PCR products were separated on 1.5% agarose gels and visualized by EtBr staining.

Quantitative real-time RT-PCR was performed essentially as described (39). The oligonucleotide primers and probes for the *OGG1* and β-actin genes were purchased from Applied Biosystems (Assays-on-Demand™). Quantitative measurements of each mRNA level were performed in triplicate. The accuracy of mRNA quantitation for each gene was confirmed by measurement of serially diluted control mRNA samples and comparison of the fluorescent intensity from a standard carve of the mRNA levels. Amplification of β-actin mRNA was performed with all samples to control the variation in mRNA levels. The gene expression levels were normalized to β-actin levels for each mRNA preparation, and the -fold increase in an individual gene was calculated by comparison with the result obtained without PonA stimulation. The non-template control was incubated in each amplification reaction to exclude the contaminating template.

HIV Infection and p24 Determination—PBMCs were stimulated with phytohemagglutinin for 48 h and infected with HIV-1_{MN}. HIV-1_{MN} was challenged at 100 $TCID_{50}$ (where $TCID_{50}$ is the tissue culture infectious dose resulting in 50% infected cells)/2.0–2.5 × 10^6 PBMCs or Jurkat cells for 1 h (43). These cells were washed twice with phosphate-buffered saline (PBS), and HIV-1 p24 antigen concentration in the culture supernatant was measured using a commercial kit (ZeptoMetrix Corp., Buffalo, NY).

mRNA Stability Assay—Total cellular RNA was serially prepared from Tat/293 and mTat/293 cells treated with PonA for 24 h, followed by the treatment with 2 μg/ml actinomycin D (Sigma). The amount of *OGG1* mRNA was analyzed by real-time RT-PCR as described above.

Detection of ROS—The detection of ROS was measured by flow cytometry with a FACScan (BD Biosciences) equipped with argon ion laser delivering 200 megawatts of power at 488 nm, and the results were analyzed using CellQuest™ software (BD Biosciences). After treatment of cells with PonA (10 μM) to induce Tat or mTat, the oxidation-sensitive fluorescent probe 2′,7′-dichlorofluorescein diacetate (Molecular Probes, Inc.) was added to the culture at a final concentration of 5 μM, followed by incubation at 37 °C for 30 min. The cells were washed twice with PBS, resuspended in PBS, and then subjected to the fluorescence-activated cell sorter detection of 5,6-carboxy-2′,7′-dichlorofluorescein (green) at 530 nm.

Measurement of Intracellular Reduced GSH and GSSG Contents—The total cellular GSH and GSSG concentrations were measured using a glutathione quantification kit (Dojindo). Briefly, each cell culture (5 × 10^6 cells) was centrifuged at 2000 × *g* for 5 min, and the cell pellet was resuspended in 100 μl of PBS. The cell suspension was treated with 80 μl of 10 mM HCl, crashed by freeze/thawing repeated twice, and further treated by adding 20 μl of 5% sulfosalicylic acid to precipitate the proteins. The supernatant was obtained by centrifugation at 10,000 × *g* for 10 min, and the total GSH and GSSG concentrations were determined. The sample was incubated with GSH reductase and NADPH at 30 °C for 5 min, and the total GSH concentration thus generated was measured by reaction with 5,5′-dithiobis(2-nitrobenzoic acid) at 30 °C for 10 min. Spectrophotometric detection of 5-mercapto-2-nitrobenzoic acid was performed at 415 nm. The GSSG concentration was determined by performing the same procedure, but GSH was masked by treatment with 2-vinylpyridine and triethanolamine prior to the reaction with GSH reductase and NADPH. The concentration of reduced GSH was determined by subtracting the GSSG concentration from the total GSH concentration. Each determination was performed in triplicate, and experiments were repeated at least twice.

Measurement of Manganese Superoxide Dismutase Activity—The enzymatic activity of manganese superoxide dismutase was measured using a WST-1™ superoxide dismutase assay kit (Dojindo) with slight modifications. Briefly, equal numbers of cells (1.5 × 10^7) were washed twice with PBS, and the cell lysates were extracted by freeze/thawing. The manganese superoxide dismutase activity in the supernatant protein lysate was determined by incubation with WST-1, xanthine, and xanthine oxidase at 37 °C for 20 min. To mask the copper superoxide dismutase and zinc superoxide dismutase activities, the protein lysate was treated with 1 mM KCN. The inhibitory action of manganese superoxide dismutase contained in each cell lysate was assessed by the spectrophotometric determination of WST-1 formazan at 450 nm. Quantitation was achieved by comparison with the absorption of standard manganese superoxide dismutase (Sigma) with known concentrations.

Electrophoretic Mobility Shift Assay—The experimental procedure was carried out as described previously (36). The AP-4 consensus sequence was taken from the 5′-AP-4 site in the *OGG1* promoter. The wild-type and mutant oligonucleotide sequences (sense strand) utilized were as follows: wild-type, 5′-CGG CAG GCA GCA GCT GTG GCG G-3′; and mutant, 5′-CGG CAG GCA GTC GCG ATG GCG G-3′. These oligonucleotides were labeled using a 5′-end labeling kit (Takara) in the presence [γ-^{32}P]dATP (Amersham Biosciences). DNA binding reactions were performed at 4 °C for 20 min in a 10-μl reaction volume. Analysis of binding complexes was performed by electrophoresis on 6% polyacrylamide gels with 0.5× Tris borate/EDTA buffer, followed by autoradiography. The specificity of DNA binding was assessed by preincubating extracts with anti-AP-4 antibody and competitor at room temperature for 10 min.

Chromatin Immunoprecipitation (ChIP) Assay—ChIP assay was performed according to the recommendations of Upstate Biotechnology, Inc., with some modification. Briefly, cells were cross-linked with 1% formaldehyde for 10 min at room temperature, washed twice with ice-cold PBS, and lysed for 10 min at 2 × 10^6 cells in 200 μl of SDS lysis buffer. The chromatin was sheared by sonication 13 times for 10 s at one-third of the maximum power with 20 s of cooling on ice between each pulse. Cross-linked released chromatin fractions were precleared with salmon sperm DNA and protein A-agarose beads for 1 h, followed by immunoprecipitation overnight with the desired antibodies at 4 °C. The immunoprecipitates were sequentially washed once with lysis buffer, twice with high salt buffer, twice with low salt buffer, and twice with Tris/EDTA buffer. After the wash, immune complexes were collected with salmon sperm DNA and protein A-agarose beads at room temperature for 1 h and extracted with 1% SDS and 0.1 M $NaHCO_3$. The eluted samples were reverse-cross-linked with proteinase K at 65 °C for 6 h and treated with RNase at 37 °C for 1 h. DNA was recovered by phenol/chloroform and chloroform extraction and ethanol precipitation. Finally, DNA was dissolved in 30 μl of Tris/EDTA buffer and subjected to PCR. The primer sequences were as follows: *OGG1* promoter (−615 to −450), 5′-CAA ACG TCC CAT TCC GAG GAA AG-3′ (forward) and 5′-GGC CTT TAG GCG TCC TCT GAG A-3′ (reverse); and β-actin promoter (−980 to −915; used as a control), 5′-TGC ACT GTG CGG CGA AGC-3′ (forward) and 5′-TCG AGC CAT AAA AGG CAA-3′ (reverse). The number of PCR cycles was as follows: 33 PCR cycles for all ChIP experiments and 25 PCR cycles for the input samples, in which PCR amplification was performed under the linear range of AP-4 binding to the *OGG1* promoter. For each reaction, 10% of the cross-linked released chromatin was saved and reversed by proteinase K digestion at 65 °C for 6 h, followed by DNA extraction; and the recovered DNA was used as input control.

Measurement of 8-Oxo-dG—The amounts of 8-oxo-dG in the cellular DNA were measured using a high performance liquid chromatography (HPLC)-electrochemical detector (ECD) system, which is highly selec-

tive, with sensitivity at the femtomole level, as described previously (26, 44). Briefly, cellular DNA was isolated using a DNA extractor WB kit (Wako Pure Chemical Industries, Osaka, Japan). The isolated DNA was digested with P1 nuclease (Wako Pure Chemical Industries) to obtain 8-oxo-dG in the nucleoside form (8-hydroxydeoxyguanosine). The nucleoside solution was filtered with an Ultrafree Probind filter (Millipore Corp.) and injected into an HPLC column (CAPCELL PAK C_{18} MG, Shiseido, Tokyo, Japan) equipped with an ECD (Coulochem II, ESA, Inc.) at a flow rate of 0.8 ml/min with the mobile phase consisting of 10 mM Na_2HPO_4 and 8% methanol. The 8-oxo-dG value in the DNA was calculated as the number of 8-oxo-dG residue/10^6 dG residues.

RNA Interference—siRNA with two thymidine residues (dTdT) at the 3′-end of the sequence was synthesized by Takara. The target sequences were as follows: OGG1 No. 1, 5′-GCC UUC UGG ACA AUC UUU C-3′; OGG1 No. 2, 5′-GCC UUC UGG ACA AUC UUU C-3′; OGG1 No. 3, 5′-GGC UCA GAA AUU CCA AGG U-3′; and green fluorescent protein, 5′-GGC UAC GUC CAG GAG CGC ACC-3′. Transfection of siRNA was performed using Lipofectamine 2000 reagent (Invitrogen). Cells were incubated for 72 h and harvested for the analysis of 8-oxo-dG and OGG1 protein expression.

RESULTS

Establishment and Characterization of Ecdysone-inducible Cell Lines Expressing Tat and mTat—Because Tat is known to impair cell viability and its activity in long-term maintenance of cells expressing Tat may preselect certain cell types and preclude exploration of the Tat-mediated alteration of cellular functions, we adopted a stringent ecdysone-inducible system using PonA, a phytoecdysteroid that is inert in mammals (45). To generate Tat- or mTat-expressing cells upon treatment with PonA, we transfected the pIND-Tat or pIND-mTat plasmid into HEK293-EcR cells stably transfected with pVgRXR expressing the receptor for ecdysone (PonA). These cells were singly isolated by two successive rounds of limiting dilution and screened for expression of Tat proteins and their transcriptional activity in stimulating HIV gene expression.

As shown in Fig. 1*A*, the expression of Tat and mTat proteins was detected after 12 h of PonA treatment and was maintained for at least an additional 60 h. (PonA dose-dependent Tat expression is also shown.) In Fig. 1*B*, Tat-mediated HIV-1 transactivation was examined. As expected, Tat (but not mTat) augmented HIV-1 gene expression in a PonA dose-dependent manner. Fig. 1*C* shows that Tat (but not mTat) bound to endogenous cyclin T1 in cells as reported previously (6–8). These results indicate that both Tat/293 and mTat/293 cells inducibly express Tat proteins and that the functional integrity of Tat is maintained in Tat/293 cells. Thus, we explored the gene expression profile in these cells.

Gene Expression Profile Analysis of Cells Expressing Tat—To identify genes either up-regulated or down-regulated by Tat in the newly established ecdysone-inducible cell lines, the gene expression profiles were compared with and without Tat expression. The mRNA was isolated from Tat/293 and Lac Z/293 cells without (control) and with PonA treatment. The cDNA probes were synthesized from each mRNA, labeled with Cy5 (for Tat- or LacZ-expressing cells) or Cy3 (for non-expressing cells), and hybridized to a gene chip (human 3K DNA CHIP™). Representative results are shown in Fig. 2*A*, where we compared genes expressed in Tat-expressing (Cy5-labeled) and non-expressing control (Cy3-labeled) 293/Tat cells. Similar comparisons were made with LacZ-expressing cells (data not shown).

As shown in Fig. 2*A*, 12 genes, including *TFPI2*, stanniocalcin-1, *SEPP1*, and *OGG1*, were up-regulated by >2-fold by Tat after 24 h of induction upon PonA treatment. Five of these 12 genes were up-regulated by >2-fold even after 12 h of Tat induction. The details of these genes are summarized in Table I. In control LacZ/293 cells, expression of the *TFPI2* gene was up-regulated by 2.0-fold when cells were treated with PonA, suggesting nonspecific stimulation by PonA (data not shown). On the other hand, eight genes were down-regulated to <60% after 24 h of Tat induction (summarized in Table II). Down-regulation of these genes was not observed in LacZ-expressing cells (data not shown).

To confirm these results, we carried out RT-PCR analysis to examine the mRNA levels of Tat-regulated genes before and after Tat induction. We also examined the effect of mTat to further confirm the specificity of Tat action. Fig. 2*B* shows the results of eight genes up-regulated by Tat by >2.3-fold (stanniocalcin-1, *SEPP1*, *OGG1*, *MEN1β2* homolog FLJ23538/clone 137308, *ETV5*, *SLC20A1*, integrin α7, and *ENPP2*; excluding *TFPI2*). Among these genes, stanniocalcin-1, *SEPP1*, and *ETV5* were also up-regulated by induction of mTat or even LacZ, suggesting a nonspecific effect of PonA. Thus, we concluded that five genes (*OGG1*, *MEN1β2* homolog FLJ23538/clone 137308, integrin α7, *SLC20A1*, and *ENPP2*) are specifically up-regulated by Tat because these genes were not up-regulated by either mTat or LacZ. Whereas *ENPP2* was up-regulated after 12–24 h of Tat induction and subsequently down-regulated, the other four genes were constitutively up-regulated.

Similarly, RT-PCR analysis was performed with the eight genes down-regulated by Tat (Fig. 2*C*). Two of the genes (*SLC1A3* and *LTA1*) were down-regulated by mTat or LacZ. The other six genes were down-regulated by Tat, but not by mTat or LacZ. Among the genes down-regulated by Tat, *NDRG1*, *RGS16*, and hexokinase-2 are known to be under the transcriptional control of p53 (46–48), an observation consistent with previous reports of Tat down-regulating the action of p53 (49, 50).

Induction of OGG1 Gene Expression by Tat—Because Tat up-regulated the *OGG1* gene the most, we further analyzed the effect of Tat on *OGG1* mRNA expression and stability. The human *OGG1* gene encodes two isoforms, type 1 (a and b) and type 2 (a, b, and c), resulting from alternative splicing of the single *OGG1* precursor mRNA (51). As shown in Fig. 3*A*, Tat induced all types of *OGG1* mRNA. We carried out real-time RT-PCR to determine more precisely the mRNA levels of *OGG1* before and after Tat induction. As shown in Fig. 3*B*, *OGG1* gene expression was up-regulated by 3.6-, 6.7-, 9.8-, and 8.2-fold upon Tat expression after 6, 12, 24, and 48 h of PonA treatment, respectively. mTat did not affect *OGG1* gene expression (Fig. 3*B*). A similar extent of stimulation was observed for OGG1 protein levels as revealed by Western blotting (Fig. 3*C*). No induction of OGG1 protein was observed when mTat was induced. Induction of OGG1 protein by Tat (but not mTat) was confirmed in Jurkat T cells, a natural host of HIV-1 infection (Fig. 3*C*, *right panels*). Furthermore, the effect of HIV-1 infection on *OGG1* gene expression was examined with PBMCs isolated from two individuals and Jurkat cells. These cells were infected with HIV-1_{MN}, and the *OGG1* mRNA level was quantified by real-time RT-PCR together with the amounts of HIV-1 produced in the culture supernatant. As shown in Fig. 3*D*, up-regulation of *OGG1* mRNA levels upon HIV-1 infection was observed and was associated with elevation of viral p24 antigen levels. Mock infection did not induce *OGG1* expression (data not shown).

Furthermore, we examined the effect of Tat on the stability of *OGG1* mRNA using PonA-inducible cells. After 24 h of Tat or mTat induction, cells were treated with actinomycin D, and total RNA samples were obtained after 1, 3, 5, and 7 h of actinomycin D treatment to determine the level of *OGG1* mRNA. As shown in Fig. 3*E*, the decay profiles of *OGG1* mRNA were similar in cells expressing Tat and mTat (control), with half-lives of 5.0 and 4.3 h, respectively. These findings indicate that the positive effects of Tat on *OGG1* gene expression are at the level of transcription.

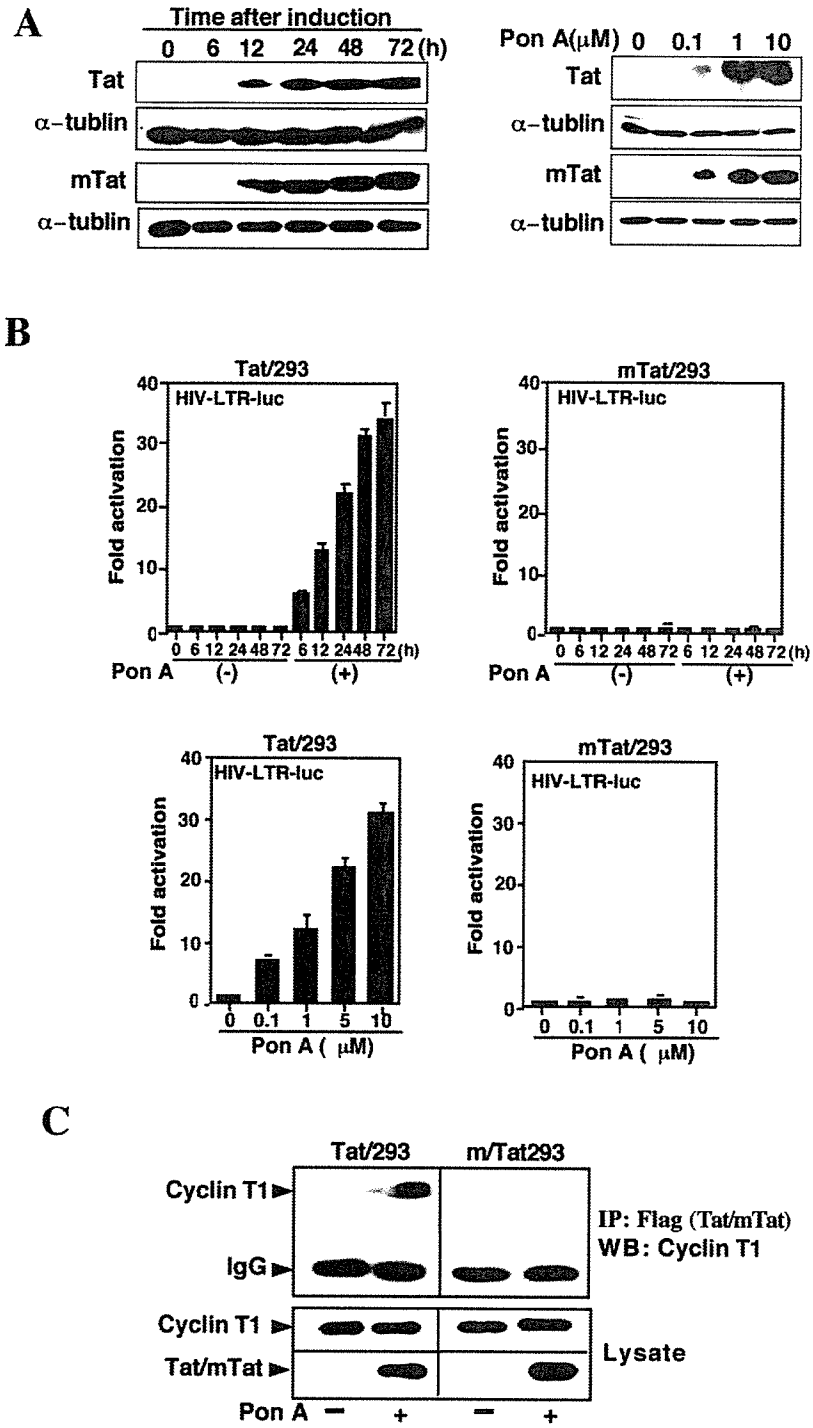

FIG. 1. **Ecdysone-inducible cell lines expressing Tat and mTat.** *A*, inducible expression of Tat and mTat. Tat/293 and mTat/293 cells were treated with PonA (10 μM) for the indicated periods of time (*left panels*) at the indicated concentrations (*right panels*). The FLAG-tagged Tat and mTat proteins were detected by Western blotting with anti-FLAG antibody. Anti-α-tubulin antibody was used to indicate that the equivalent amount of protein from each cell lysate was loaded. *B*, Tat-mediated transactivation of HIV-1 gene expression. Tat/293 (*left panels*) and mTat/293 (*right panels*) cells were transfected with HIV-1 long terminal repeat (*LTR*)-luciferase (*luc*), maintained in culture for 24 h, and then treated for the indicated periods of time with 10 μM PonA (*upper panels*) or for 48 h with various concentrations of PonA (*lower panels*). *C*, co-immunoprecipitation of cyclin T1 with Tat. Tat/293 and mTat/293 cells were treated with PonA for 24 h, and the cell lysates were immunoprecipitated (*IP*) with anti-FLAG antibody (detecting Tat). Immune complexes were collected and subjected to SDS-PAGE, followed by Western blotting (*WB*) with anti-cyclin T1 antibody. One-tenth of each protein lysate used in each reaction was loaded as the input control.

Induction of OGG1 Expression Is Not through the Oxidative Stress Induced by Tat—Because Tat is known to induce oxidative stress (12, 15, 17), it is possible that *OGG1* induction might be an indirect effect of Tat, although it is not yet known whether oxidative stress induces *OGG1* gene expression. We first examined whether Tat induces oxidative stress in Tat/293 cells. Fluorescence-activated cell sorter analysis with the oxidation-sensitive fluorescent probe 2′,7′-dichlorofluorescein diacetate showed that Tat (but not mTat) increased the intracellular ROS levels (Fig. 4*A*). We measured the intracellular levels of GSH and GSSG. As expected, the content of GSSG, the oxidized form of GSH, was increased (~2.3-fold) in Tat-expressing cells in contrast to control mTat-expressing cells (Fig. 4*B*). The GSH (reduced form) level in Tat-expressing cells was decreased to 57% of that in control cells. No significant reduction in GSH was detected in mTat-expressing cells. Furthermore, the manganese superoxide dismutase activity was down-regulated by Tat as reported previously (12). After 24 h of Tat induction, the manganese superoxide dismutase activity was decreased to 59% (Fig. 4*C*).

These results led us to examine whether Tat-induced *OGG1* gene expression is attributable to the oxidative stress associated with Tat action. However, treatment with antioxidants did not block Tat-mediated *OGG1* induction (Fig. 4*D*). 293/Tat cells were pretreated with antioxidants, including pyrrolidine dithiocarbamate, *N*-acetyl-L-cysteine, epigallocatechin gallate (a phenolic antioxidant), and Trolox (a water-soluble vitamin E analog), prior to Tat induction (Fig. 4*D*, *left panel*). When the *OGG1* mRNA was measured by real-time RT-PCR, Tat-induced *OGG1* expression was not affected by the antioxidants. In

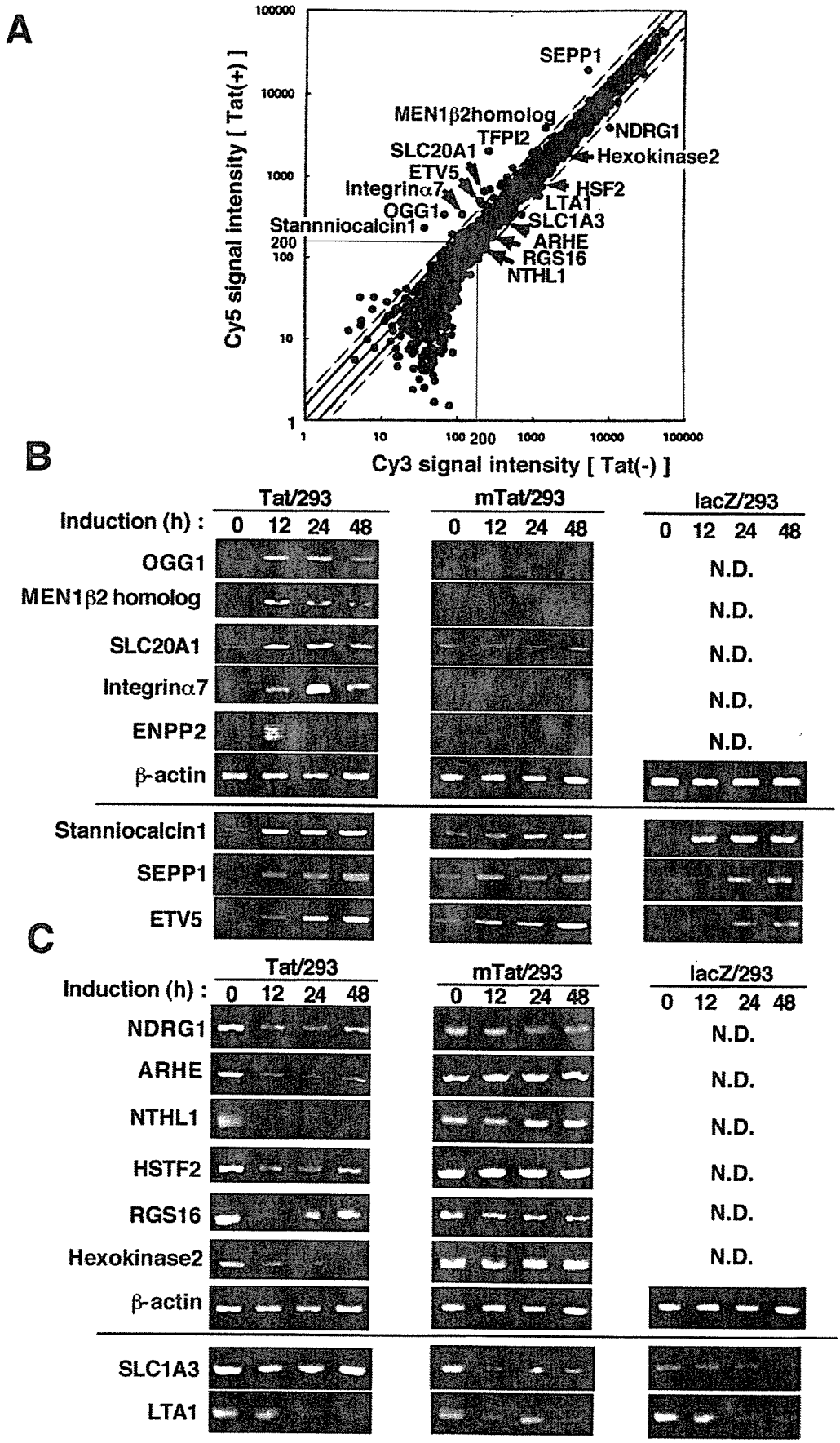

FIG. 2. **Gene expression profile analysis and confirmatory RT-PCR.** *A*, scatter plot of the hybridization signal intensity of genes in cells expressing Tat *versus* control cells. The mRNA was isolated from Tat/293 cells without (control) or with PonA treatment for 24 h. The cDNA probes were synthesized from the mRNA of each cell culture and labeled with either Cy5 (for Tat-expressing cells) or Cy3 (for control 293 cells). These probes were hybridized, in combination, to a gene chip (human 3K DNA CHIP™). The signal intensity of each gene on the microarray chip was

TABLE I
Genes up-regulated by Tat

Gene	Induction		GenBank™ accession no.
	12 h	24 h	
	-fold		
TFPI2[a]	6.5[b]	7.9 ± 0.7[c]	NM_006528
Stanniocalcin-1[a]	2.4	4.0 ± 0.3	NM_003155
SEPP1[a]	2.4	3.4 ± 0.3	NM_005410
OGG1	2.6	2.7 ± 0.2	NM_016819
Human clone 137308 mRNA; similar to *MEN1β*$_2$[d]	1.1	2.7 ± 0.2	U60873
ETV5 (Ets-related molecule)[a]	1.8	2.6 ± 0.2	NM_004454
Homo sapiens cDNA, similar to *MEN1β*$_2$[d]	1.1	2.5 ± 0.2	AK027191
SLC20A1	1.8	2.5 ± 0.3	NM_005415
Integrin α7	1.9	2.4 ± 0.1	NM_002206
ENPP2/autotaxin	1.7	2.3 ± 0.2	NM_006209
ABCG1 (ATP-binding cassette, subfamily G (WHITE), member 1)	1.3	2.1 ± 0.1	NM_004915
Calcium-binding protein p22	2.1	2.0 ± 0.1	BC001646
Laminin α3	1.4	2.0 ± 0.1	NM_000227

[a] Nonspecifically up-regulated by PonA treatment (see Fig. 2 for the results of RT-PCR).
[b] Data from single determinations 12 h after Tat induction.
[c] Data from triplicate determinations 24 h after Tat induction (expressed as means ± S.D.).
[d] Different cDNA segments of the same gene.

TABLE II
Genes down-regulated by Tat

Gene	Induction		GenBank™ accession no.
	12 h	24 h	
	-fold		
NDRG1	0.5[a]	0.4 ± 0.1[b]	NM_006096
ARHE	0.5	0.5 ± 0.1	NM_005168
SLC1A3[c]	0.7	0.5 ± 0.1	NM_004172
NTHL1	0.8	0.6 ± 0.1	NM_002528
HSTF2	0.5	0.6 ± 0.1	NM_004506
RGS16	0.7	0.6 ± 0.1	NM_002928
Hexokinase-2	0.7	0.6 ± 0.1	NM_000189
LTA1[c]	1.3	0.6 ± 0.2	AF104032

[a] Data from single determinations 12 h after Tat induction.
[b] Data from triplicate determinations 24 h after Tat induction (expressed as means ± S.D.).
[c] Nonspecifically up-regulated by PonA treatment (see Fig. 2 for the results of RT-PCR).

addition, H_2O_2 and oxidative stress inducers such as inflammatory cytokines (tumor necrosis factor-α and interleukin-1β) and lipopolysaccharide could not up-regulate *OGG1* gene expression (Fig. 4*D*, *right panel*). In support of these findings, when we performed transient luciferase assay using the *OGG1* promoter construct, no *OGG1* induction by these stimuli was observed (data not shown), consistent with a previous report by Dhénaut *et al.* (37). Therefore, it is unlikely that Tat induces *OGG1* expression through ROS production.

Transactivation of OGG1 by Tat—These observations prompted us to examine the possibility that Tat-mediated *OGG1* expression is the direct effect of Tat. We thus examined the effect of Tat on *OGG1* promoter activity. The transient luciferase assay was performed on various regions of the *OGG1* promoter linked to the luciferase reporter gene (Fig. 5). As shown in Fig. 5*A*, Tat stimulated the transcriptional activity of the reporter constructs containing the sequence upstream from position −472. Whereas the sequence upstream from position −945 was dispensable for Tat-mediated transactivation, no such effect was observed when the region spanning positions −945 to −472 was deleted (Fig. 5*A*, *lower left panel*). In 293 cells expressing mTat, no induction of *OGG1* promoter activity (other than the constitutive transcriptional activity) was observed. We also examined the Tat-mediated transactivation of the *OGG1* promoter in Jurkat cells and obtained essentially the same results (Fig. 5*A*, *lower right panel*).

Thus, Tat appears to transactivate *OGG1* expression through transcription factors located within the *OGG1* promoter region from positions −945 to −472. To further elucidate the mechanism by which Tat induces *OGG1* transcription, we created specific mutants lacking binding sites for GATA, AP-4, and/or AP-2 located in this region. When AP-4 sites were mutated, Tat no longer augmented the promoter activity (Fig. 5*B*, *black bars*). However, no reduction in Tat-mediated transactivation was observed when other sites were mutated. In addition, the basal promoter activity was augmented when the 5′-AP-4 site was mutated, whereas mutation of the GATA, AP-2, and 3′-AP-4 sites had little effect on the basal *OGG1* promoter activity (Fig. 5*B*, *hatched bars*), indicating that AP-4 acts as a transcriptional repressor of *OGG1* expression. These results suggest that AP-4 sites are required for Tat-induced *OGG1* gene expression and that the 5′-AP-4 site negatively regulates *OGG1* gene expression. In fact, overexpression of AP-4 inhibited both the Tat-stimulated and basal levels of *OGG1* gene expression without affecting the level of Tat expression (Fig. 5*C*).

Tat Interacts with AP-4 and Removes It from the OGG1 Promoter—To further investigate the mechanism by which Tat stimulates *OGG1* gene expression, we first examined the effect of Tat on AP-4 DNA binding by electrophoretic mobility shift assay. As shown in Fig. 6*A*, constitutive AP-4 DNA binding was observed in the cells, and a significant reduction in AP-4 DNA binding was observed when Tat was induced by PonA treatment. No such effect was observed when mTat was expressed. We then examined whether Tat associates with AP-4 in cultured cells by co-immunoprecipitation with either Tat (FLAG epitope-tagged) or AP-4 (Myc epitope-tagged). As shown in Fig. 6*B*, when Tat was immunoprecipitated with anti-FLAG antibody, endogenous AP-4 protein was detected within the immune complex. No AP-4 was co-immunoprecipitated with mTat. Conversely, when AP-4 was immunoprecipitated with

plotted. Genes with a signal intensity <200 U (of Cy5 and Cy3) were excluded from further analysis. *Solid* and *dashed lines* indicate the upper and lower boundaries of 1.5- and 2.0-fold changes, respectively. *B* and *C*, confirmation of genes up- or down-regulated by Tat using RT-PCR. *B*, genes up-regulated by Tat. Up-regulation of the stanniocalcin-1, *SEPP1*, and *ETV5* genes observed in cDNA array analysis appeared to be unspecific. *C*, genes down-regulated by Tat. Down-regulation of the *SLC1A3* and *LTA1* genes was considered nonspecific. RT-PCR analysis was performed with gene-specific primers and total RNA prepared from Tat/293, mTat/293, and LacZ/293 cells. Each cell culture was treated with PonA (10 μM) for the indicated periods of time. *N.D.*, not determined.

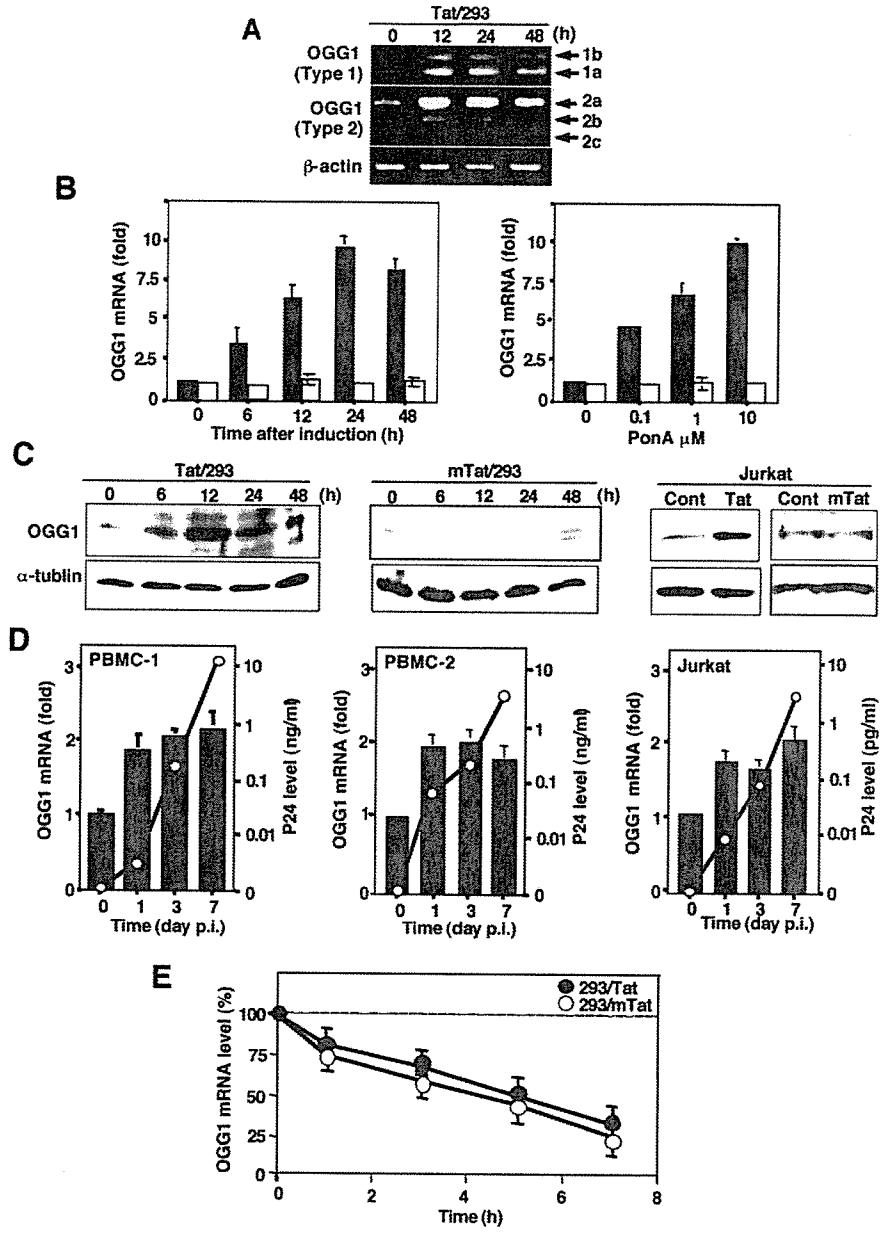

FIG. 3. **Induction of OGG1 by Tat.** *A*, induction of *OGG1* mRNA species by Tat. Tat/293 cells were treated with PonA (10 μM) for the indicated periods of time. RT-PCR analysis was performed with specific primers for the *OGG1* type 1 and 2 genes. Note that all of the splicing variants of *OGG1* mRNA were similarly up-regulated by Tat. *B*, quantitation of *OGG1* mRNA induction by real-time RT-PCR analysis. Tat/293 (*black bars*) and mTat/293 (*white bars*) cells were treated with 10 μM PonA for the indicated periods of time (*left panel*) or for 24 h with various concentrations of PonA (*right panel*). The total RNA was purified from each culture preparation and subjected to real-time RT-PCR using an *OGG1* primer/probe mixture. *C*, induction of OGG1 protein by Tat. Tat/293 (*left panel*) and mTat/293 (*middle panel*) cells were treated with PonA (10 μM) for the indicated periods of time, and OGG1 proteins were examined by Western blotting with anti-OGG1 antibody. Jurkat cells (*right panel*) were transfected with pcDNA-Tat, pcDNA-mTat, or the control (*Cont*) plasmid for 24 h. *D*, induction of *OGG1* mRNA by HIV-1 infection. PBMCs from two individuals and Jurkat cells were infected with HIV-1_{MN} at 100 $TCID_{50}$, and the *OGG1* RNA levels were measured by real-time RT-PCR. HIV-1 production was measured by the viral p24 antigen level in the culture supernatants. *p.i.*, post-infection in days. *E*, effect of Tat on *OGG1* mRNA stability. Tat/293 and mTat/293 cells were treated with PonA (10 μM) for 24 h and treated with actinomycin D (2 μg/ml). Total cellular RNA was obtained at the indicated time points, and the amount of *OGG1* mRNA was determined by real-time RT-PCR analysis. The experiments were performed in triplicate.

anti-Myc antibody, Tat (but not mTat) was co-immunoprecipitated (Fig. 6*B*, *lower panels*).

Furthermore, the ChIP assay was performed to examine whether the inhibition of AP-4 DNA binding by Tat occurs at the endogenous *OGG1* gene promoter. Tat/293 and mTat/293 cells were transfected with plasmids expressing Myc-tagged AP-4 or Myc-tagged LacZ (control), stimulated with PonA to express Tat or mTat, treated with formamide, and sonicated, and the cross-linked protein·DNA complex was immunoprecipitated with specific antibodies recognizing the Myc (AP-4) or V5 (Tat) epitope. The immunoprecipitated DNA was analyzed by PCR using primer pairs for the AP-4-binding sites within the *OGG1* promoter (−615 to −450). As demonstrated in Fig. 6*C*, a significant reduction in AP-4 bound to the *OGG1* promoter DNA was observed, and the extent of reduction was proportionate to the amount of Tat expressed (corresponding to the time-dependent expression of Tat in Fig. 1). No such effect was observed when mTat was expressed. The antibody to Tat precipitated the *OGG1* promoter (Fig. 6*C*, *left panels*), indicating that the Tat·AP-4·DNA ternary complex may be transiently formed. These observations indicate that Tat directly activates *OGG1* gene expression through sequestrating AP-4, a negative transcriptional regulator of *OGG1* expression.

Reduction of 8-Oxo-dG Levels by Tat and Effect of OGG1 Knockdown—Because OGG1 is responsible for the excision/repair of the oxidation-damaged DNA by excising 8-oxo-dG (30) and because Tat induces expression of OGG1, we measured the amounts of 8-oxo-dG in the cellular DNA by the HPLC-ECD method (26). Fig. 7*A* shows the levels of 8-oxo-dG before and after Tat expression. In control cells, the level of 8-oxo-dG was 8.7 ± 0.34 residues/10^6 dG residues (Fig. 7*B*). However, upon expression of Tat, the 8-oxo-dG levels were reduced to 7.7 ± 1.6 (0.89-fold), 5.6 ± 0.30 (0.64-fold), and 4.5 ± 1.2 (0.52-fold) residues/10^6 dG residues after 6, 12, and 24 h of Tat induction, respectively. Statistically significant reduction was observed after 12 and 24 h of Tat induction. No significant reduction in 8-oxo-dG levels was observed when mTat was expressed. Taken together, these observations indicate that Tat prevents accumulation of 8-oxo-dG by directly up-regulating OGG1 expression.

To confirm these findings, we adopted a siRNA technique to specifically knock down *OGG1* mRNA and examined the effect of Tat on the level of 8-oxo-dG when endogenous OGG1 was

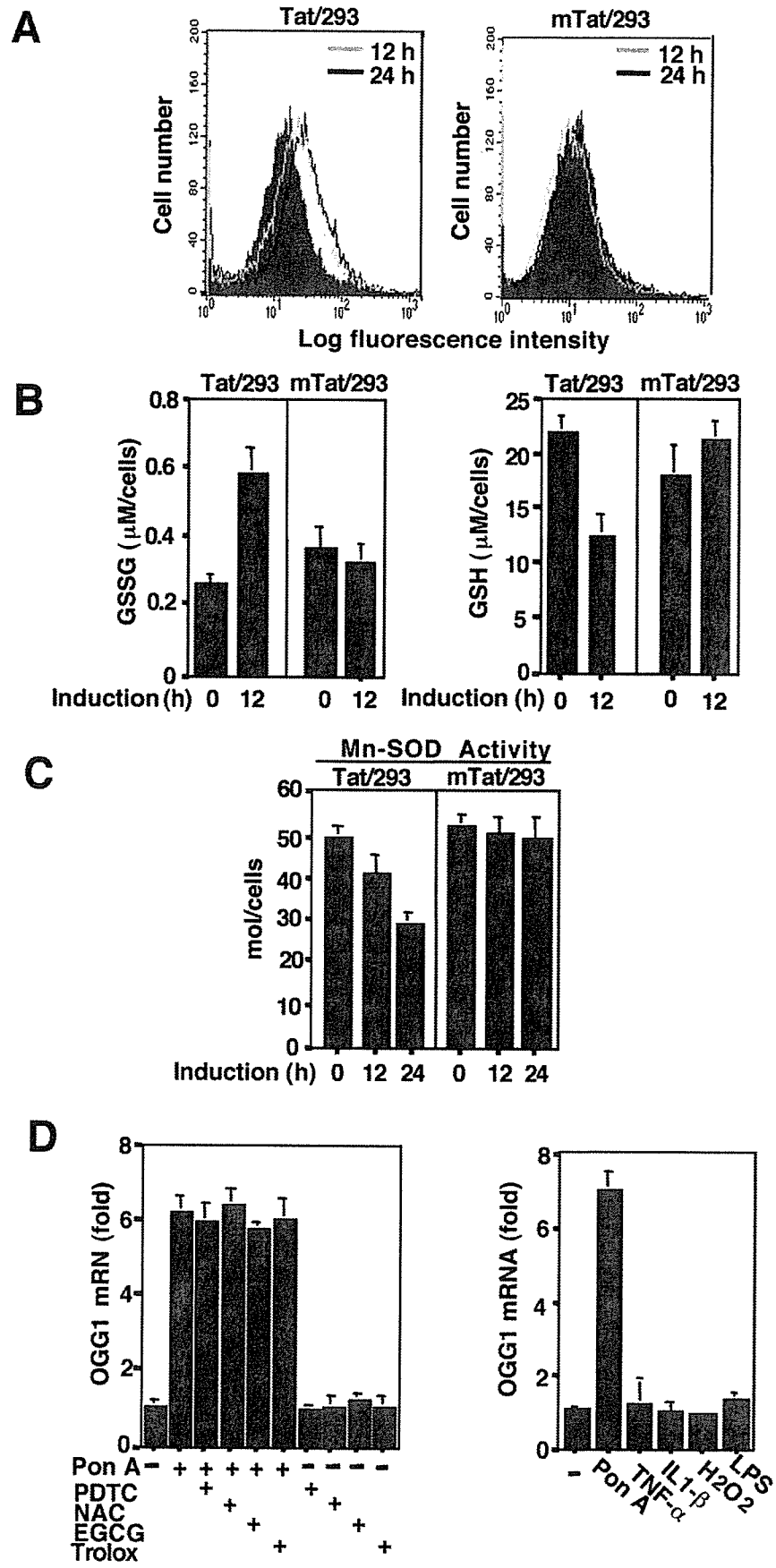

FIG. 4. **Induction of oxidative stress by Tat and effects of antioxidants on Tat-mediated *OGG1* expression.** *A*, accumulation of ROS by Tat. Tat/293 (*left panel*) and mTat/293 (*right panel*) cells were treated with 5 μM 2′,7′-dichlorofluorescein diacetate for 30 min, followed by treatment with PonA (10 μM) for 12 or 24 h. The intracellular 5,6-carboxy-2′,7′-dichlorofluorescein level (the indicator for ROS) in the cells was measured by flow cytometry. *B*, changes in GSSG (*left panel*) and GSH (*right panel*) contents by Tat. Tat/293 and mTat/293 cells were treated with PonA at 10 μM for 12 h, and GSH and GSSG contents were determined by the 5,5′-dithiobis(2-nitrobenzoic acid)/GSH reductase recycling method. To measure the GSSG content, GSH was masked by treatment with 2-vinylpyridine and triethanolamine prior to the reaction with GSH reductase and NADPH. *C*, inhibition of manganese superoxide dismutase (*Mn-SOD*) activity by Tat. Tat/293 and mTat/293 cells were treated with PonA (10 μM) for 12 or 24 h. The lysates were treated with KCN to mask copper superoxide dismutase and zinc superoxide dismutase activities, and then the manganese superoxide dismutase activity was measured by enzymatic assay. *D*, effects of various antioxidants on Tat-induced *OGG1* expression. Total RNA was prepared from each cell culture, and *OGG1* mRNA was quantitated by real-time RT-PCR as described in the legend to Fig. 2*B*. *Left panel*, Tat/293 cells were pretreated for 1 h with pyrrolidine dithiocarbamate (*PDTC*; 100 μM), *N*-acetyl-L-cysteine (*NAC*; 20 mM), epigallocatechin gallate (*EGCG*; 20 μM), or Trolox (100 μM) and stimulated with PonA (10 μM) for 12 h, and total RNA was prepared. *Right panel*, Tat/293 cells were treated with tumor necrosis factor-α (*TNF-α*; 5 ng/ml), interleukin-1β (*IL-1β*; 10 ng/ml), H_2O_2 (1 mM), lipopolysaccharide (*LPS*; 200 ng/ml), or PonA (10 μM) for 12 h, and the *OGG1* RNA levels were measured.

depleted. We synthesized three kinds of 21-nucleotide siRNA duplexes corresponding to the conserved *OGG1* mRNA region utilized in all types of *OGG1* mRNA species. Cells transduced with OGG1 siRNA (No. 1) showed the greatest reduction in OGG1 protein levels compared with the control (Fig. 7*C*) and were thus used in the following experiment. As demonstrated

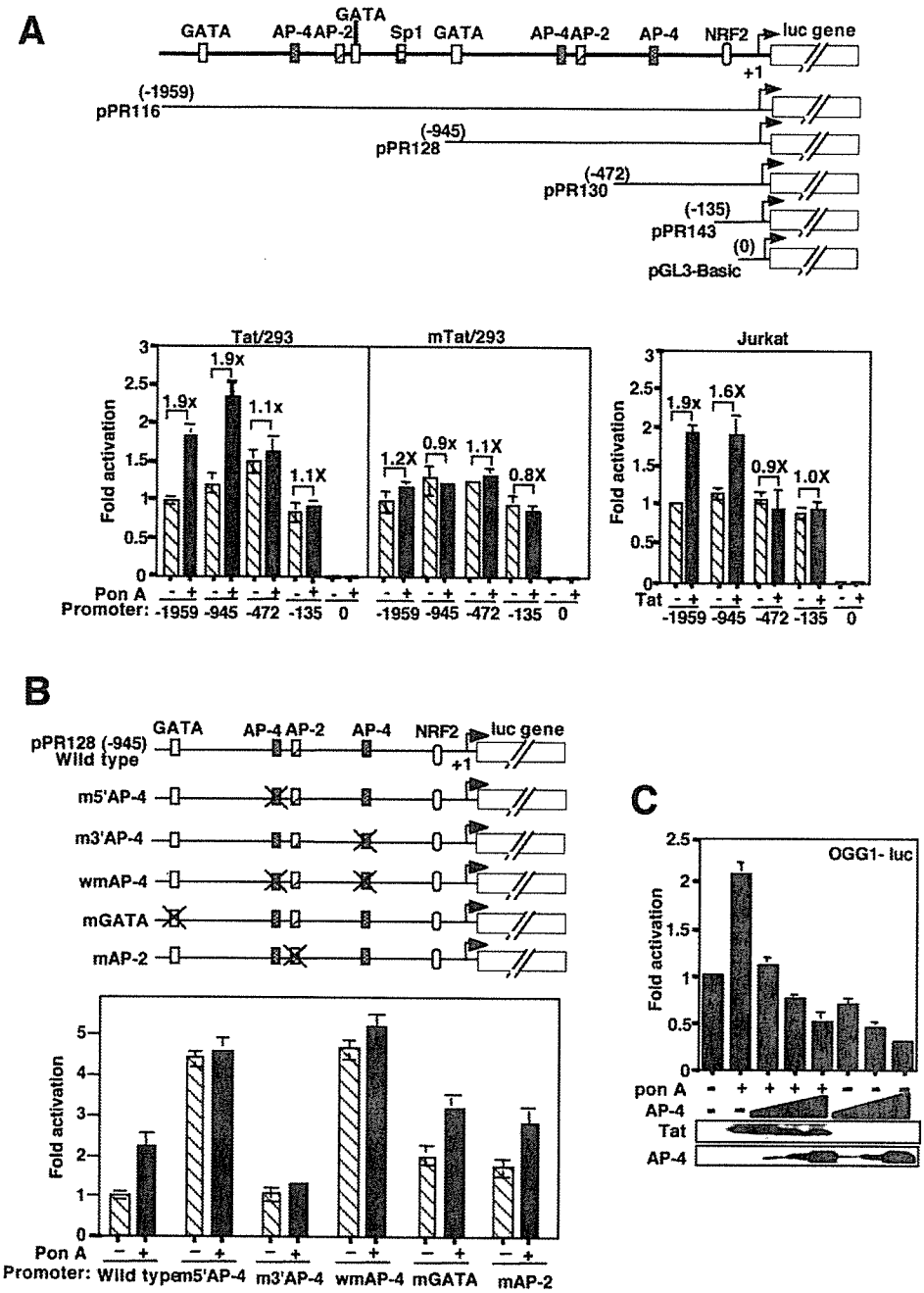

FIG. 5. **Tat directly activates *OGG1* gene expression.** *A*, effect of Tat on *OGG1* promoter activity. Schematic diagrams of the *OGG1* promoter constructs are shown, indicating the positions of various *cis*-elements for transcription factors GATA, AP-4, AP-2, Sp1, and NRF2 (nuclear factor erythroid-related factor 2) (*upper panel*). Tat/293 and mTat/293 cells (*lower left panel*) were transfected with various *OGG1* promoter constructs, incubated for 24 h, and treated (*black bars*) or not (*hatched bars*) with PonA (10 μM) for an additional 24 h. Jurkat cells (*lower right panel*) were transfected with *OGG1* promoter constructs in the presence (*black bars*) or absence (*hatched bars*) of pcDNA-Tat. Cells were harvested, and the luciferase (*luc*) activity was measured. The data are presented as the -fold increase in luciferase activity (means ± S.D.) relative to the transcriptional activity of the full-length *OGG1* promoter (pPR116) from three independent experiments. *B*, involvement of AP-4 in Tat-mediated *OGG1* expression. Various mutations in the binding sites for GATA, AP-4, and AP-2 were introduced into a wild-type *OGG1* promoter (pPR128-luc), and the effects of Tat were examined. Schematic representations of wild-type and mutant pPR128-luc constructs are shown (*upper panel*). Tat/293 cells were transfected with these reporter constructs, and the effects of Tat were similarly examined (*lower panel*). Note the increase in basal promoter levels with mutants containing a substitution in the 5′-AP-4 site and the lack of Tat response in mutants containing 5′- and/or 3′-AP-4 sites. *C*, repression of *OGG1* expression by AP-4. Tat/293 cells were transfected with pPR116-luc together with various amounts of plasmid expressing Myc-AP-4, incubated for 24 h, and treated with PonA (10 μM) for an additional 24 h to induce Tat expression (*upper panel*). The dose-dependent expression of AP-4 was revealed by Western blotting with anti-Myc tag antibody (*lower panels*). Tat protein expression was monitored using anti-FLAG antibody.

in Fig. 7*D*, OGG1 depletion by OGG1 siRNA (No. 1) resulted in a significant increase in the level of 8-oxo-dG (1.6-fold with the control and 1.4-fold with control siRNA). More important, 8-oxo-dG formation was induced by Tat when OGG1 was depleted (2.2-fold with the control and 1.9-fold with control siRNA). In addition, overexpression of AP-4, acting as a negative regulator of *OGG1* expression, increased the level of 8-oxo-dG (1.8-fold with the control).

DISCUSSION

In this study, we have explored the biological effects of Tat using gene expression profile analysis. We found that (i) Tat induces the *OGG1* gene and that (ii) Tat down-regulates the *NDRG1*, *RSG16*, and hexokinase-2 genes. The latter genes are known to be under the transcriptional control of p53 (46–48). Interestingly, Li *et al.* (49) observed the repression of p53 mRNA by Tat. Moreover, Tat was shown to directly inactivate p53 by protein-protein interaction (50, 52). Thus, the Tat-mediated down-regulation of these genes is consistent with previous findings. However, Tat-mediated OGG1 induction has not been reported. Thus, in this study, we analyzed the mechanism by which Tat induces *OGG1* gene expression.

We found that Tat-mediated OGG1 induction is not through stabilization of the *OGG1* mRNA. In addition, Tat-mediated *OGG1* induction was not reversed by treatment with antioxidants, indicating that Tat-mediated *OGG1* induction could not be attributable to oxidative stress induced by Tat. By performing transient luciferase assay using the reporter plasmid containing various regions of *OGG1*, we found that Tat induces *OGG1* gene expression through the central AP-4 site (located at positions −545 to −540) in its upstream region. Although AP-4 is known to activate expression of the SV40 (53) and transforming growth factor-β (54) genes, it is also known to repress expression of the human angiotensinogen (55) and HIV-1 (56) genes, although the mechanism of AP-4 action has not been clarified. Our experiments have revealed that AP-4 negatively regulates *OGG1* gene expression via binding to the central

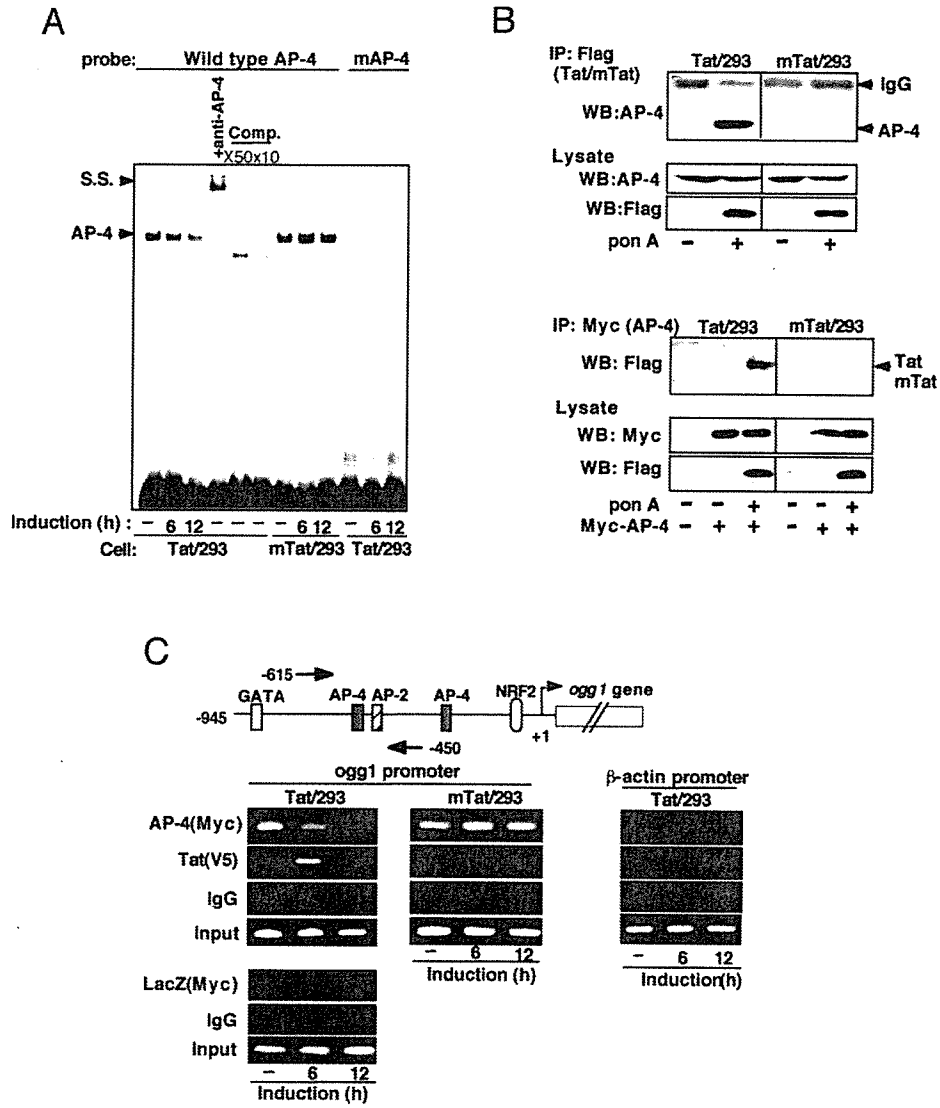

FIG. 6. **Mechanism by which Tat induces *OGG1* gene expression: Tat interacts with AP-4 and removes AP-4 from the *OGG1* promoter.** *A*, effect of Tat on AP-4 DNA binding. Nuclear extracts were prepared from Tat/293 and mTat/293 cells, and AP-4 DNA binding was examined by electrophoretic mobility shift assay using AP-4 or mutant AP-4 probes. To verify the AP-4·DNA complex, nuclear extracts were incubated with anti-AP-4 antibody or excess amounts of competitor oligonucleotides (10- or 50-fold). The positions of the specific protein·DNA and supershifted (*S.S.*) complexes (*arrowheads*) are indicated. *B*, interaction between Tat and AP-4 *in vivo*. *Upper panel*, cell lysates were prepared, and immune complexes containing Tat or mTat were immunoprecipitated (*IP*) with anti-FLAG antibody (detecting Tat). The immunoprecipitates were separated by SDS-PAGE, followed by Western blotting (*WB*) with anti-AP-4 antibody. One-tenth of each protein lysate used in each reaction was loaded as the input control. *Lower panels*, Tat/293 and mTat/293 cells were transfected with plasmid expressing Myc-AP-4, and expression of Tat proteins was induced by PonA (10 μM). The cell lysates were immunoprecipitated with anti-Myc antibody (detecting AP-4), and the immune complex was analyzed for the presence of Tat by Western blotting with anti-FLAG antibody. *C*, ChIP assay. *Upper panel*, the *OGG1* promoter region amplified by the primer pairs in ChIP assay is illustrated. *Arrows* indicate the positions of PCR primers. *Lower panels*, cell lysates were prepared from Tat/293 and mTat/293 cells that were transfected with plasmid expressing Myc-AP-4 or Myc-LacZ (control) and treated with PonA (10 μM) for expression of Tat and mTat. Cross-linked chromatin fragments were prepared, and the association of AP-4, LacZ, Tat, and *OGG1* promoter DNA was analyzed by ChIP assay. The recovered DNA was amplified by PCR with promoter-specific primers and analyzed on a 2% agarose gel. DNAs isolated from sonicated cross-linked chromatin fragments were used as inputs. The β-actin promoter DNA was similarly analyzed as a control.

AP-4 site and that Tat activates *OGG1* promoter activity by sequestrating AP-4 from the *OGG1* promoter. Thus, the positive effect of Tat on *OGG1* gene expression appears to be a direct effect.

Intriguingly, we observed that the extent of oxidation-induced guanosine modification (8-oxo-dG) was reduced, although Tat induced oxidative stress as revealed by the increase in ROS and GSSG and the decrease in manganese superoxide dismutase activity. When OGG1 expression was knocked down by siRNA, the amount of 8-oxo-dG was increased, suggesting that the Tat-induced reduction of 8-oxo-dG requires *OGG1* gene expression and that the Tat-mediated induction of OGG1 appears to be independent of Tat pro-oxidant action.

Thus, in addition to its crucial role in viral replication, Tat appears to play a role in maintenance of the genetic integrity of proviral and host cell DNAs. Although various conditions associated with HIV infection and replication are pro-oxidant (12, 13, 57–59), the observed mutations accumulated within the HIV genome have been revealed to be in favor of the G:C to A:T transition (18–22) rather than the G:C to T:A transversion mediated by the oxidative modification. This is in contrast with most of the mutations associated with human cancers, where the G:C to T:A transversion is predominant (28, 29). If induction of OGG1 were through oxidative stress associated with Tat actions, the level of 8-oxo-dG should have been higher in Tat-expressing cells than in control cells. These findings indicate that Tat-mediated OGG1 induction is more than a feedback action. Although additional studies are needed, such as the

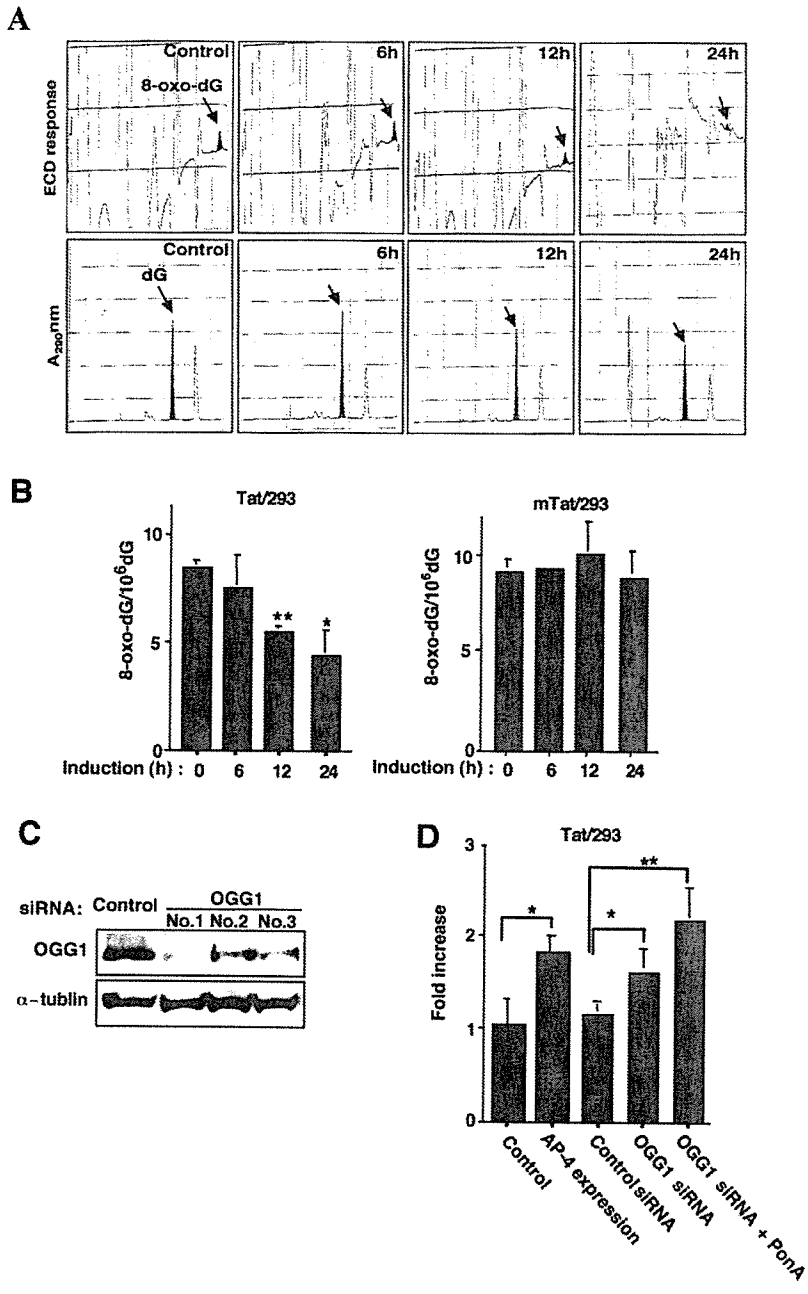

FIG. 7. **Reduction in the levels of 8-oxo-dG by Tat.** *A*, electrochemical chromatographs of 8-oxo-dG. The HPLC patterns were traced using an ECD. The 8-oxo-dG peaks (ECD response; *shaded areas* in the *upper panels*) are indicated by *arrows*. The dG peaks (absorption at 290 nm; *shaded areas* in the *lower panels*) are also indicated. Cells were treated for the indicated periods of time with PonA (10 μM) to express Tat or mTat. Nuclear DNA samples were prepared and measured for 8-oxo-dG levels. DNA was digested to obtain deoxynucleosides and analyzed with an HPLC-ECD system as described under "Experimental Procedures." *B*, levels of 8-oxo-dG in DNA expressing Tat or mTat. The amount of 8-oxo-dG is expressed as the number of 8-oxo-dG residues/10^6 dG residues. The results represent the means ± S.D. from four independent experiments. *, $p < 0.005$; **, $p < 0.001$. *C*, OGG1 knockdown by siRNA. Tat/293 cells were transfected with 100 nM siRNAs directed against various portions of OGG1 (Nos. 1–3) or green fluorescent protein (control) mRNAs. After 72 h of transfection, cells were lysed, and OGG1 protein levels were assessed by Western blotting with anti-OGG1 antibody (*upper panel*). The blot was stripped and reprobed with anti-α-tubulin antibody (*lower panel*). *D*, effects of OGG1 depletion and expression of Tat and AP-4 on the levels of 8-oxo-dG. *First bar*, control Tat/293 cells (no treatment); *second bar*, Tat/293 cells transfected with plasmid expressing AP-4; *third* and *fourth bars*, Tat/293 cells transfected with siRNA against green fluorescent protein (siRNA control) or OGG1 (No. 1), respectively, and incubated for 72 h; *fifth bar*, Tat/293 cells transfected with siRNA against OGG1 (No. 1) for 48 h and treated with PonA to induce Tat expression for an additional 24 h. At 72 h post-transfection, nuclear DNA samples were extracted, and the levels of 8-oxo-dG were measured similarly as described for *A*. The levels of 8-oxo-dG are shown as the -fold increase compared with the level of the no-treatment sample (*first bar*). *, $p < 0.05$; **, $p < 0.01$.

effect of OGG1 mutation on the extent of mutation of viral and cellular genomes during chronic HIV infection, the Tat-mediated induction of OGG1 could be viewed as a regulated "feed-forward" mechanism.

Acknowledgments—We thank Drs. J. P. Radicella and L. Naumovski for providing the plasmid constructs containing various portions of the *OGG1* promoter and 293/LacZ cells, respectively. We also thank A. Victoriano for language revision.

REFERENCES

1. Jones, K. A., and Peterlin, B. M. (1994) *Annu. Rev. Biochem.* **63,** 717–743
2. Berkhout, B., Silverman, R. H., and Jeang, K. T. (1989) *Cell* **59,** 273–282
3. Okamoto, T., and Wong-Staal, F. (1986) *Cell* 29–35
4. Okamoto, H., Sheline, C. T., Corden, J. L., Jones, K. A., and Peterlin, B. M. (1996) *Proc. Natl. Acad. Sci. U. S. A.* **93,** 11575–11579
5. Wei, P., Garber, M. E., Fang, S. M., Fischer, W. H., and Jones, K. A. (1998) *Cell* **92,** 451–462
6. Kanazawa, S., Okamoto, T., and Peterlin, B. M. (2000) *Immunity* **12,** 61–70
7. Mancebo, H. S., Lee, G., Flygare, J., Tomassini, J., Luu, P., Zhu, Y., Peng, J., Blau, C., Hazuda, D., Price, D., and Flores, O. (1997) *Genes Dev.* **11,** 2633–2644
8. Zhu, Y., Pe'ery, T., Peng, J., Ramanathan, Y., Marshall, N., Marshall, T., Amendt, B., Mathews, M. B., and Price, D. H. (1997) *Genes Dev.* **11,** 2622–2632
9. Marzio, G., Tyagi, M., Gutierrez, M. I., and Giacca, M. (1998) *Proc. Natl. Acad. Sci. U. S. A.* **95,** 13519–13524
10. Price, D. H. (2000) *Mol. Cell. Biol.* **20,** 2629–2634
11. Zauli, G., Gibellini, D., Milani, D., Mazzoni, M., Borgatti, P., La Placa, M., and Capitani, S. (1993) *Cancer Res.* **53,** 4481–4485
12. Flores, S. C., Marecki, J. C., Harper, K. P., Bose, S. K., Nelson, S. K., and McCord, J. M. (1993) *Proc. Natl. Acad. Sci. U. S. A.* **90,** 7632–7636
13. Westendorp, M. O., Shatrov, V. A., Schulze-Osthoff, K., Frank, R., Kraft, M., Los, M., Krammer, P. H., Droge, W., and Lehmann, V. (1995) *EMBO J.* **14,** 546–554
14. Conant, K., Garzino-Demo, A., Nath, A., McArthur, J. C., Halliday, W., Power, C., Gallo, R. C., and Major, E. O. (1998) *Proc. Natl. Acad. Sci. U. S. A.* **95,** 3117–3121
15. Izmailova, E., Bertley, F. M., Huang, Q., Makori, N., Miller, C. J., Young, R. A., and Aldovini, A. (2003) *Nat. Med.* **9,** 191–197
16. Choi, J., Liu, R. M., Kundu, R. K., Sangiorgi, F., Wu, W., Maxson, R., and Forman, H. J. (2000) *J. Biol. Chem.* **275,** 3693–3698
17. Kumar, A., Manna, S. K., Dhawan, S., and Aggarwal, B. B. (1998) *J. Immunol.* **161,** 776–781
18. Li, Y., Kappes, J. C., Conway, J. A., Price, R. W., Shaw, G. M., and Hahn, B. H. (1991) *J. Virol.* **65,** 3973–3985
19. Moriyama, E. N., Ina, Y., Ikeo, K., Shimizu, N., and Gojobori, T. (1991) *J. Mol. Evol.* **32,** 360–363
20. Perry, S. T., Flaherty, M. T., Kelley, M. J., Clabough, D. L., Tronick, S. R., Coggins, L., Whetter, L., Lengel, C. R., and Fuller, F. (1992) *J. Virol.* **66,** 4085–4097
21. Vartanian, J. P., Meyerhans, A., Asjo, A., and Wain-Hobson, S. (1991) *J. Virol.* **65,** 1779–1788
22. Harris, R. S., Bishop, K. N., Sheehy, A. M., Craig, H. M., Petersen-Mahrt,

S. K., Watt, I. N., Neuberger, M. S., and Malim, M. H. (2003) *Cell* **113,** 803–809
23. Mangeat, B., Turelli, P., Caron, G., Friedli, M., Perrin, L., and Trono, D. (2003) *Nature* **424,** 99–103
24. Mariani, R., Chen, D., Schrofelbauer, B., Navarro, F., Konig, R., Bollman, B., Munk, C., Nymark-McMahon, H., and Landau, N. R. (2003) *Cell* **114,** 21–31
25. Zhang, H., Yang, B., Pomerantz, R. J., Zhang, C., Arunachalam, S. C., and Gao, L. (2003) *Nature* **424,** 94–98
26. Kasai, H., and Nishimura, S. (1984) *Nucleic Acids Res.* **12,** 2137–2145
27. Kasai, H. (1997) *Mutat. Res.* **387,** 147–163
28. Hatahet, Z., Zhou, M., Reha-Krantz, L. J., Morrical, S. W., and Wallace, S. S. (1998) *Proc. Natl. Acad. Sci. U. S. A.* **95,** 8556–8561
29. Hussain, S. P., and Harris, C. C. (1998) *Cancer Res.* **58,** 4023–4037
30. Boiteux, S., and Radicella, J. P. (2000) *Arch. Biochem. Biophys.* **377,** 1–8
31. Radicella, J. P., Dherin, C., Desmaze, C., Fox, M. S., and Boiteux, S. (1997) *Proc. Natl. Acad. Sci. U. S. A.* **94,** 8010–8015
32. Rosenquist, T. A., Zharkov, D. O., and Grollman, A. P. (1997) *Proc. Natl. Acad. Sci. U. S. A.* **94,** 7429–7434
33. Arai, T., Kelly, V. P., Komoro, K., Minowa, O., Noda, T., and Nishimura, S. (2003) *Cancer Res.* **63,** 4287–4292
34. Minowa, O., Arai, T., Hirano, M., Monden, Y., Nakai, S., Fukuda, M., Itoh, M., Takano, H., Hippou, Y., Aburatani, H., Masumura, K., Nohmi, T., Nishimura, S., and Noda, T. (2000) *Proc. Natl. Acad. Sci. U. S. A.* **97,** 4156–4161
35. Okamoto, H., Cujec, T. P., Okamoto, M., Peterlin, B. M., Baba, M., and Okamoto, T. (2000) *Virology* **272,** 402–408
36. Takada, N., Sanda, T., Okamoto, H., Yang, J. P., Asamitsu, K., Sarol, L., Kimura, G., Uranishi, H., Tetsuka, T., and Okamoto, T. (2002) *J. Virol.* **76,** 8019–8030
37. Dhénaut, A., Boiteux, S., and Radicella, J. P. (2000) *Mutat. Res.* **461,** 109–118
38. Ao, Y., Rohde, L. H., and Naumovski, L. (2001) *Oncogene* **20,** 2720–2725
39. Ando, K., Kanazawa, S., Tetsuka, T., Ohta, S., Jiang, X., Tada, T., Kobayashi, M., Matsui, N., and Okamoto, T. (2003) *Oncogene* **22,** 7796–7803
40. Watanabe, N., Ando, K., Yoshida, S., Inuzuka, S., Kobayashi, M., Matsui, N., and Okamoto, T. (2002) *Biochem. Biophys. Res. Commun.* **294,** 1121–1129
41. Tetsuka, T., Uranishi, H., Imai, H., Ono, T., Sonta, S., Takahashi, N., Asamitsu, K., and Okamoto, T. (2000) *J. Biol. Chem.* **275,** 4383–4390
42. Sarol, L. C., Imai, K., Asamitsu, K., Tetsuka, T., Barzaga, N. G., and Okamoto, T. (2002) *Biochem. Biophys. Res. Commun.* **291,** 890–896
43. Pincus, S. H., Messer, K. G., and Hu, S. H. (1994) *J. Clin. Investig.* **93,** 140–146
44. Tsurudome, Y., Hirano, T., Yamato, H., Tanaka, I., Sagai, M., Hirano, H., Nagata, N., Itoh, H., and Kasai, H. (1999) *Carcinogenesis* **20,** 1573–1576
45. Saez, E., Nelson, M. C., Eshelman, B., Banayo, E., Koder, A., Cho, G. J., and Evans, R. M. (2000) *Proc. Natl. Acad. Sci. U. S. A.* **97,** 14512–14517
46. Buckbinder, L., Velasco-Miguel, S., Chen, Y., Xu, N., Talbott, R., Gelbert, L., Gao, J., Seizinger, B. R., Gutkind, J. S., and Kley, N. (1997) *Proc. Natl. Acad. Sci. U. S. A.* **94,** 7868–7872
47. Kurdistani, S. K., Arizti, P., Reimer, C. L., Sugrue, M. M., Aaronson, S. A., and Lee, S. W. (1998) *Cancer Res.* **58,** 4439–4444
48. Mathupala, S. P., Heese, C., and Pedersen, P. L. (1997) *J. Biol. Chem.* **272,** 22776–22780
49. Li, C. J., Wang, C., Friedman, D. J., and Pardee, A. B. (1995) *Proc. Natl. Acad. Sci. U. S. A.* **92,** 5461–5464
50. Longo, F., Marchetti, M. A., Castagnoli, L., Battaglia, P. A., and Gigliani, F. (1995) *Biochem. Biophys. Res. Commun.* **206,** 326–334
51. Nishioka, K., Ohtsubo, T., Oda, H., Fujiwara, T., Kang, D., Sugimachi, K., and Nakabeppu, Y. (1999) *Mol. Biol. Cell.* **10,** 1637–1652
52. Clark, E., Santiago, F., Deng, L., Chong, S., de La Fuente, C., Wang, L., Fu, P., Stein, D., Denny, T., Lanka, V., Mozafari, F., Okamoto, T., and Kashanchi, F. (2000) *J. Virol.* **74,** 5040–5052
53. Mermod, N., Williams, T. J., and Tjian, R. (1988) *Nature* **332,** 557–561
54. Andriamanalijaona, R., Felisaz, N., Kim, S. J., King-Jones, K., Lehmann, M., Pujol, J. P., and Boumediene, K. (2003) *Arthritis Rheum.* **48,** 1569–1581
55. Cui, Y., Narayanan, C. S., Zhou, J., and Kumar, A. (1998) *Gene (Amst.)* **224,** 97–107
56. Ou, S. H., Garcia-Martinez, L. F., Paulssen, E. J., and Gaynor, R. B. (1994) *J. Virol.* **68,** 7188–7199
57. Staal, F. J., Ela, S. W., Roederer, M., Anderson, M. T., Herzenberg, L. A., and Herzenberg, L. A. (1992) *Lancet* **339,** 909–912
58. Roederer, M., Staal, F. J., Raju, P. A., Ela, S. W., Herzenberg, L. A., and Herzenberg, L. A. (1990) *Proc. Natl. Acad. Sci. U. S. A.* **87,** 4884–4888
59. Kalebic, T., Kinter, A., Poli, G., Anderson, M. E., Meister, A., and Fauci, A. S. (1991) *Proc. Natl. Acad. Sci. U. S. A.* **88,** 986–990

Eur. J. Biochem. **271**, 3741–3751 (2004) © FEBS 2004 doi:10.1111/j.1432-1033.2004.04314.x

RNA helicase A interacts with nuclear factor κB p65 and functions as a transcriptional coactivator

Toshifumi Tetsuka[1], Hiroaki Uranishi[1], Takaomi Sanda[1], Kaori Asamitsu[1], Jiang-Ping Yang[2], Flossie Wong-Staal[2] and Takashi Okamoto[1]

[1]*Department of Molecular and Cellular Biology, Nagoya City University Graduate School of Medical Sciences, Nagoya, Aichi, Japan;* [2]*Department of Medicine, University of California San Diego, La Jolla, CA, USA*

RNA helicase A (RHA), a member of DNA and RNA helicase family containing ATPase activity, is involved in many steps of gene expression such as transcription and mRNA export. RHA has been reported to bind directly to the transcriptional coactivator, CREB-binding protein, and the tumor suppressor protein, BRCA1, and links them to RNA Polymerase II holoenzyme complex. Using yeast two-hybrid screening, we have identified RHA as an interacting molecule of the p65 subunit of nuclear factor κB (NF-κB). The interaction between p65 and RHA was confirmed by glutathione-*S* transferase pull-down assay *in vitro*, and by co-immunoprecipitation assay *in vivo*. In transient transfection assays, RHA enhanced NF-κB dependent reporter gene expression induced by p65, tumor necrosis factor-α, or NF-κB inducing kinase. The mutant form of RHA lacking ATP-binding activity inhibited NF-κB dependent reporter gene expression induced by these activators. Moreover, depletion of RHA using short interfering RNA reduced the NF-κB dependent transactivation. These data suggest that RHA is an essential component of the transactivation complex by mediating the transcriptional activity of NF-κB.

Keywords: coactivator; NF-κB; protein–protein interaction; RNA helicase A; transcription.

Nuclear factor κB (NF-κB) is an inducible cellular transcription factor that regulates a wide variety of cellular and viral genes including cytokines, cell adhesion molecules and HIV [1–3]. The members of the NF-κB family in mammalian cells include the proto-oncogene c-Rel, RelA (p65), RelB, NFkB1 (p50/105), and NFkB2 (p52/p100). In most cells, Rel family members form hetero- and homodimers with distinct specificities in various combinations. p65, RelB and c-Rel are transcriptionally active members of the NF-κB family, whereas p50 and p52 serve primarily as DNA binding subunits [1–3]. These proteins play fundamental roles in immune and inflammatory responses and in the control of cell proliferation [4,5]. A common feature of the regulation of NF-κB is their sequestration in the cytoplasm as an inactive complex with a class of inhibitory molecules known as IκBs. Treatment of cells with a variety of inducers such as interleukin-1 (IL-1) and tumor necrosis factor (TNF) results in phosphorylation, ubiquitination and degradation of the IκB proteins [1–3].

The protein regions responsible for the transcriptional activation [called 'transactivation (TA) domain'] of p65, Rel B and c-Rel have been mapped in their unique C-terminal regions. p65 contains at least two independent TA domains within its C-terminal 120 amino acids (Fig. 1A). One of these TA domains, TA1, is confined to the C-terminal 30 amino acids of p65. The second TA domain, TA2, is localized in the N-terminally adjacent 90 amino acids and contains TA1-like motif. As the nuclear translocation and DNA binding of NF-κB were not sufficient for gene induction [6,7], it was suggested that interactions with other protein molecules through the TA domain [8–10] as well as its modification by phosphorylation [11–14] might play critical roles in the NF-κB-mediated gene expression.

It has been shown that NF-κB requires multiple coactivator proteins including CREB-binding protein (CBP)/p300 [8–10,15,16], CBP associated factor, and steroid receptor coactivator 1 [17]. These proteins have histone acetyl transferase activity that modifies chromatin structure and provides molecular bridges to the basal transcriptional machinery. p65 was also found to interact with a newly identified coactivator complex, activator-recruited cofactor/vitaminD receptor-interacting protein, which potentiated chromatin-dependent transcriptional activation by NF-κB *in vitro* [18]. Aside from coactivators, the transcriptional activity of gene-specific activators can also be mediated by general transcription factors.

Correspondence to T. Okamoto, Department of Molecular and Cellular Biology, Nagoya City University Graduate School of Medical Sciences, 1 Kawasumi, Mizuho-cho, Mizuho-ku, Nagoya, Aichi 467–8601, Japan. Fax: +81 52 859 1235, Tel.: +81 52 853 8204, E-mail: tokamoto@med.nagoya-cu.ac.jp

Abbreviations: AD, (transcriptional) activation domain; AES, amino-terminal enhancer of split; CREB, cAMP response element binding protein; CBP, CREB-binding protein; CMV, cytomegalovirus; DBD, DNA-binding domain; GIR, Groucho-interacting region; Grg, Groucho-related genes; GST, glutathione-*S* transferase; ICAM-1, intercellular adhesion molecule-1; IFN-β, interferon-β; IL-1, interleukin-1; MLE, maleless; MSL, male-specific lethal; NF-κB, nuclear factor κB; NIK, NF-κB inducing kinase; NLS, nuclear localization signal; RAI, RelA-associated inhibitor; RHA, RNA helicase A; RNA Pol II, RNA polymerase II; TLE1, transducin-like enhancer of split 1; TLS, translocated in liposarcoma; TNF-α, tumor necrosis factor-α.

(Received 8 April 2004, revised 15 July 2004, accepted 30 July 2004)

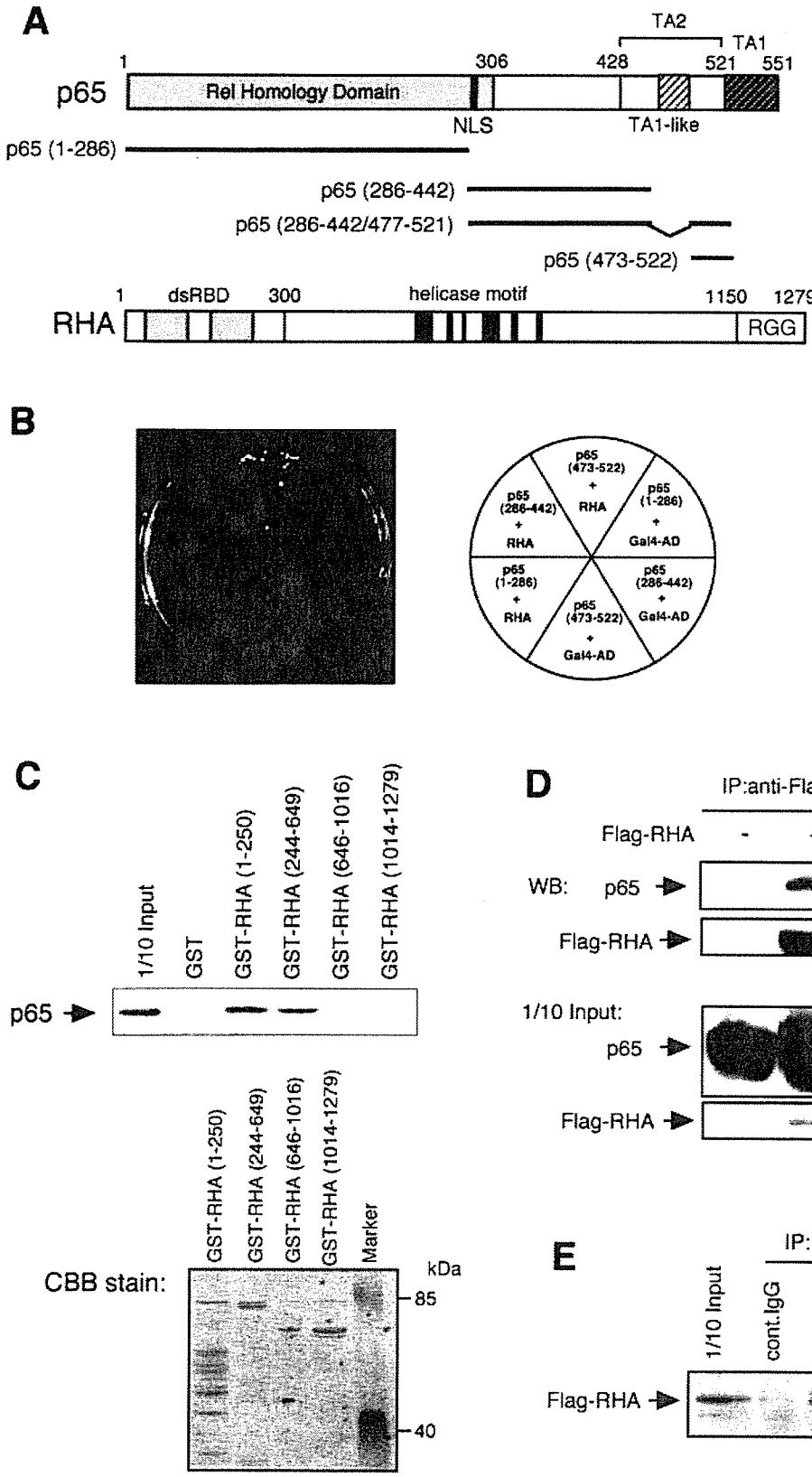

In the case of NF-κB, the association of p65 with general transcription factors such as TFIIB, $TAF_{II}105$, and TBP has been demonstrated [8,19–22]. It is thus postulated that specific protein–protein interactions with NF-κB determine its transcriptional competence. Up-regulation of the NF-κB transcriptional activity is mediated by interaction with basal factors and coactivators while its down-regulation is mediated by interaction with inhibitors and corepressors at

Fig. 1. Interaction between p65 and RHA. (A) Schematic illustrations of various functional domains of p65 and RHA. dsRBD, double stranded RNA-binding domain; NLS, nuclear localization signal; TA1, transactivation domain 1; TA2, transactivation domain 2 (containing TA1-like domain, Groucho-interacting region, and leucine-rich region); RGG, Arg-Gly-Gly rich region. (B) Growth of yeast transformants coexpressing p65 and RHA on the selective medium. The yeast Y190 was transformed with pACT2-RHA and pGBT plasmids expressing various portions of the p65 in fusion with Gal4-DBD. The yeast transformants grown on plates lacking Leu and Trp were streaked on plates lacking Leu, Trp and His, and containing 25 mM 3-aminotriazole. (C) p65 binds to RHA *in vitro*. p65 was labeled with [^{35}S]-methionine by *in vitro* transcription/translation. Radiolabeled p65 was incubated with GST, GST-RHA(1–250), GST-RHA(244–649), GST-RHA(646–1016) or GST-RHA(1014–1279) immobilized on glutathione-Sepharose beads. After incubation and further washing, the complexes were resolved by 10% SDS/PAGE and subjected to autoradiography. (D,E) p65 binds to RHA *in vivo*. HEK 293 cells were transfected with pCMV-p65 in combination with either pCMV-Flag-RHA or the empty vector. Whole cell extracts were harvested 48 h after transfection, and immunoprecipitated with 10 μL of anti-Flag M2 Affinity Gel, and the resulting precipitates were disrupted and immunoblotted with anti-p65 Ig and anti-Flag Ig (D, upper panel). Whole cell extracts (1/10 input) were also immunoblotted with anti-p65 Ig and anti-Flag Ig to show that the same amount of the immune complex containing p65 were loaded (D, lower panel). HEK 293 cells were transfected with pCMV-Flag-RHA and pCMV-p65 expression vectors. Whole cell extract was harvested 48 h after transfection, and RHA was immunoprecipitated with control rabbit IgG or anti-p65 rabbit polyclonal IgG. Ten microliters of protein G-agarose beads was added and the reaction was further incubated for 1 h. The immunoprecipitated proteins were resolved by 10% SDS/PAGE and immunoblotted with anti-Flag Ig (E).

multiple levels. In our previous studies, yeast two-hybrid screening yielded several novel regulators of NF-κB that interact with the p65 subunit: amino-terminal enhancer of split (AES) and transducin-like enhancer of split (TLE1) [23], both belonging to the Groucho-related genes (Grg) and acting as corepressors. The pro-oncoprotein TLS (translocated in liposarcoma), a homologue of $TAF_{II}68$, stimulates the transcriptional activity of p65 [24]. These proteins interact with a small intervening region between TA1 and TA1-like motifs, termed 'Groucho-interacting region' (GIR), within the C-terminal TA domain of p65 [23,24]. In addition, we also identified a novel nuclear protein RelA-associated inhibitor (RAI), containing ankyrin repeats and interacting with the central region of p65 that blocks the DNA binding activity of NF-κB [25,26], similar to the cytoplasmic inhibitors IκBs.

There is accumulating evidence indicating that RNA helicase A (RHA) acts as a transcriptional coactivator. RHA was found to interact with the CREB-binding protein (CBP) [27] and BRCA1 [28], and to be required for transcriptional activation. The ATP binding and/or ATP hydrolysis activities of RHA appear to be required for transcriptional activation as the RHA mutant, in which Lys417 within the conserved ATP-binding motif is substituted by Arg, resulted in the loss of RHA activity and a great reduction in transcriptional activity [27].

In this study, we demonstrate that RHA interacts directly with p65 and activates NF-κB-mediated transcription. We confirmed the interaction between p65 and RHA *in vitro* using the bacterially expressed fusion proteins and an *in vivo* co-immunoprecipitation assay. Depletion of endogenous RHA using siRNA reduced the NF-κB-mediated gene expression. These data indicate that RHA mediates the transcriptional activity of NF-κB.

Experimental procedures

Plasmids

Mammalian expression vector plasmids Gal4-Sp1, pCMV-NIK, ICAM-1-luc (−339 to −30) and E-selectin-luc, IFN-β-luc were generous gifts from S. T. Smale (UCLA School of Medicine, Los Angeles, CA, USA), D. Wallach (Weitzmann Institute of Science, Rehovot, Israel), L. A. Madge and J. S. Pober (Yale University School of Medicine, New Haven, CT, USA), and T. Taniguchi (Tokyo University, Tokyo, Japan), respectively. pCMV-RHA, pCMV-RHA-mATP, pCMV-p65, pGal4-p65, pGBT-p65(1–286), pGBT-p65(286–442), and pGBT-p65(473–522) had been described previously [23,29]. To create pACT2-RHA, the RHA cDNA was amplified by PCR using pCMV-RHA as a template with oligonucleotides containing *Bam*HI-*Xho*I site. These products were digested with *Bam*HI-*Xho*I, and subcloned in-frame into pACT2 vector at the *Bam*HI-*Sal*I site. Construction of a luciferase reporter plasmid, 4κB-luc, containing four tandem copies of the HIV-κB sequence upstream of minimal simian virus 40 (SV40) promoter had been described previously [30]. The other luciferase reporter plasmid, pGal4-luc (pFR-luc), containing five tandem copies of Gal4 binding site upstream of the TATA box, was purchased from Stratagene.

Yeast two-hybrid screening and protein–protein interaction assay

The yeast two-hybrid screening was performed as described previously [23,24,26]. The C-terminal regions of p65 corresponding to amino acids 286–442/477–521 was fused in-frame to Gal4 DNA binding domain (positions 1–147) using the pGBT9 vector (Clontech), and used as a bait for library screening. Yeast strain Y190 was transformed with pGBT-p65-(286–442/477–521) and the human placenta cDNA expression library fused to the Gal4 transactivation domain in the pACT2 vector (Clontech). Approximately one million transformants were screened for their ability to grow on the plates with medium lacking Trp, Leu, and His, and containing 25 mM 3-aminotriazole. Plasmids were rescued from clones that were positive for β-galactosidase activity and identified by nucleotide sequencing. cDNA sequences and their amino acid sequences were compared with GenBank™ and Swiss-Prot databases for identification of the interacting proteins.

Cell culture and transfection

Human embryonic kidney (HEK 293) cells were maintained in DMEM with 10% fetal bovine serum, 100 $U \cdot mL^{-1}$ of penicillin and 100 $\mu g \cdot mL^{-1}$ of streptomycin. Cells were transfected using Fugene-6 transfection reagent (Roche Molecular Biochemicals) according to the manufacturer's

instruction. At 48 h post-transfection, the cells were harvested, and the extracts were prepared for luciferase assay. Luciferase activity was measured by the Luciferase Assay System (Promega, Madison, WI) as described previously [26]. Transfection efficiency was monitored by *Renilla* luciferase activity using the pRL-TK plasmid (Promega) as an internal control. The data are presented as the fold increase in luciferase activities (mean ± SD) relative to the control of three independent transfections. Human recombinant TNF-α was purchased from Roche.

In vitro binding assay

Glutathione-*S* transferase (GST)-RHA(1–250), GST-RHA (244–649), GST-RHA(646–1016), and GST-RHA(1014–1279) were prepared as described previously [29]. These GST-RHA fusion proteins were expressed in *Escherichia coli* strain DH5α and purified. The *in vitro* protein–protein interaction assay ('pull-down' assay) was carried out as described previously [23,24,26]. The p65 protein was synthesized and labeled with [^{35}S]methionine by *in vitro* transcription/translation procedure using a TNT wheat germ extract coupled system (Promega) according to the manufacturer's protocol. Approximately 20 μg of GST fusion proteins was immobilized on 20 μL of glutathione-Sepharose beads and washed 2× with 1 mL of modified HEMNK buffer [20 mM HEPES/KOH (pH 7.5), 100 mM KCl, 12.5 mM $MgCl_2$, 0.2 mM EDTA, 0.3% NP-40, 1 mM dithiothreitol, 0.5 mM phenylmethylsulfonyl fluoride). The beads were left in 0.6 mL of HEMNK and were incubated with radiolabeled proteins for 2 h at 4 °C with gentle mixing. The beads were then washed 3× with 1 mL of HEMNK buffer and 2× with 1 mL of HEMNK buffer containing 150 mM KCl. Bound radiolabeled proteins were eluted with 30 μL of Laemmli sample buffer, boiled for 3 min, and resolved by 10% SDS/PAGE.

Co-immunoprecipitation and Western blot assays

HEK 293 cells were transfected with pCMV-p65 in combination with either CMV-Flag-RHA or the empty vector. After transfection, cells were cultured for 48 h and harvested with lysis buffer [25 mM HEPES/NaOH (pH 7.9), 150 mM NaCl, 1.5 mM $MgCl_2$, 0.2 mM EDTA, 0.3% NP-40, 5% glycerol, 1 mM dithiothreitol, 0.5 mM phenylmethylsulfonyl fluoride]. The lysates were incubated with 10 μL of anti-Flag M2 Affinity Gel (Sigma) at 4 °C for 1 h. The beads were washed 5× with 1 mL of lysis buffer. Antibody-bound complexes were eluted by boiling in Laemmli sample buffer, resolved by 10% SDS/PAGE, and transferred on nitrocellulose membrane (Hybond-C, Amersham). The membrane was incubated with anti-Flag Ig (Sigma) or anti-p65 Ig (Santa Cruz) and the immunoreactive proteins were visualized by enhanced chemiluminescence (SuperSignal, Pierce) as described previously [23,24,26]. To evaluate the level of exogenous p65 expressed from pCMV-p65 containing the His epitope-tag, rabbit polyclonal anti-$(His)_6$ Ig (Santa Cruz) was used for Western blotting.

RNA interference

The double-stranded RNA specific for RHA was synthesized by Takara Bio Inc. (Shiga, Japan). This RHA specific small interference RNA (siRNA) 5′-GCAUAAAACUUCUGC GUCU-3′ was targeted to the RHA portion from 2408 to 2426. Control siRNA 5′-AUUCUAUCACUAGCGU GAC-3′ was purchased from Dharmacon (Lafayette, CO, USA). siRNA transfections were performed using lipofectamine 2000 reagent (Invitrogen) according to the manufacturer's instruction.

Results

Identification of RHA as a p65-binding protein

To identify proteins interacting with p65 subunit of NF-κB, we performed the yeast two-hybrid screen using pGBT-p65(286–442/477–521) as a bait for the screening. Yeast strain Y 190 was used for the screening of a human placenta cDNA library fused to the Gal4 transcriptional activation domain in the pACT2 vector (Clontech). Among ≈ 1.0×10^6 Y190 yeast transformants, 90 colonies grew on selective medium and turned blue when tested with a β-galactosidase assay. Each plasmid purified from the positive colony was cotransfected with the bait plasmid into the yeast to confirm the specific interaction. DNA sequencing and comparison with GenBank and SwissProt databases revealed the gene for RHA (one clone) in addition to IκBα/MAD3 (five clones) and Bcl3 (one clone) that are known to interact with p65.

In order to map the interaction domain of p65 with RHA, we performed the yeast two-hybrid protein–protein interaction assay (Table 1, Fig. 1B). Various regions of the p65 protein were fused to Gal4-DNA binding domain in the pGBT9 vector and cotransfected with pACT2-RHA, encoding RHA fused to Gal4–transactivation domain. Interactions were tested by β-galactosidase activity (Table 1) and by growth of yeast cells on plates with medium lacking His, Leu and Trp, and containing 25 mM 3-aminotriazole (Fig. 1B). pGBT-p65(1–286), pGBT-p65(286–442), and

Table 1. Yeast two-hybrid interaction assays between p65 and RHA. Yeast Y190 cells were cotransformed with expression vectors encoding various proteins fused to Gal4 DNA-binding domain (Gal4-DBD) and Gal4 transcriptional activation domain (Gal4-AD). pACT2-RHA is a rescued clone which encodes full length RHA fused to Gal4-AD. pACT2-IκBα encodes full length IκBα (amino acids 1–317) fused to Gal4-AD. Leu^+ Trp^+ transformants were streaked on selective medium lacking Leu and Trp, and allowed to grow for 2 days at 30 °C. At least three colonies of each transformant were tested for β-galactosidase activity using X-gal colony filter assay (Clontech). +, positive for β-galactosidase activity (blue colony) after 2–3 h; –, no β-galactosidase activity (white colony) after 24 h; ND, not determined.

	Gal4-AD hybrid		
Gal4-DBD hybrid	pACT2	pACT2-RHA	pACT2-IκBα
pGBT9	–	–	–
pGBT-p65(1–286)	–	–	–
pGBT-p65(286–551)	+	ND	ND
pGBT-p65(286–521)	+	ND	ND
pGBT-p65(286–470)	+	ND	ND
pGBT-p65(286–442)	–	–	+
pGBT-p65(473–522)	–	+	–

pGBT-p65(473–522) alone did not show any background in the prototrophic selection or in the β-galactosidase assay. Among these, pGBT-p65(473–522) was shown to interact with pACT2-RHA (Table 1, Fig. 1B). These results indicate that the minimal region of p65 responsible for the interaction with RHA resides within the amino acids 473–522.

Binding of RHA to p65

To confirm the interaction between RHA and p65, we performed an *in vitro* protein–protein interaction assay using various recombinant RHA proteins in fusion with GST. The radiolabeled p65 protein was synthesized by *in vitro* transcription/translation in the presence of [^{35}S]methionine using wheat germ extract. The radiolabeled p65 was incubated with GST-RHA fusion proteins immobilized on glutathione-Sepharose beads. As shown in Fig. 1C, p65 bound to GST-RHA(1–250) and GST-RHA(244–649) but not to GST-RHA(646–1016), or GST-RHA(1014–1279). No p65 binding was detected with beads containing GST alone (as a negative control).

To investigate the interaction between RHA and p65 *in vivo*, we expressed p65 and RHA containing the Flag-epitope in the N-terminus in HEK 293 cells. Lysates were prepared from the transfected HEK 293 cells and immunoprecipitated with anti-Flag M2 Affinity Gel (Sigma) and the resulting precipitate was disrupted and immunoblotted with anti-p65 and anti-Flag Igs. As shown in Fig. 1D, p65 was co-immunoprecipitated with Flag-RHA. To confirm this interaction, the cell lysates were immunoprecipitated with anti-p65 Ig or control IgG, followed by Western blotting using anti-Flag Ig. As shown in Fig. 1E, Flag-RHA was co-immunoprecipitated with p65. These data indicate the interaction between p65 and RHA *in vivo*.

RHA mediates NF-κB-dependent gene expression

We then investigated the effect of RHA on NF-κB-dependent gene expression. In Fig. 2A, the effect of RHA was examined on gene expression from the reporter plasmid 4κB-luc by transfection of pCMV-p65 with or without cotransfection of pCMV-RHA in HEK 293 cells. RHA augmented the NF-κB-mediated transactivation in a dose-dependent manner when the p65-expression plasmid was cotransfected. pCMV-p65 alone activated gene expression from 4κB-luc, but RHA further enhanced the p65-mediated gene expression. However, there was no detectable effect of RHA on the basal transcription level in the absence of pCMV-p65. These effects of RHA was not through increasing the level of p65, as Western blot analysis of the transfected cell lysate revealed no increase in the protein level of exogenously expressed p65 (Fig. 2A, lower panel). Similarly, RHA augmented NF-κB dependent gene expression induced by TNF-α or by NF-κB inducing kinase (NIK), the upstream kinase for NF-κB activation (Fig. 2B,C).

The catalytic activity is required for the effect of RHA

To determine whether endogenous RHA is involved in NF-κB mediated transcription, we used pCMV-RHAmATP,

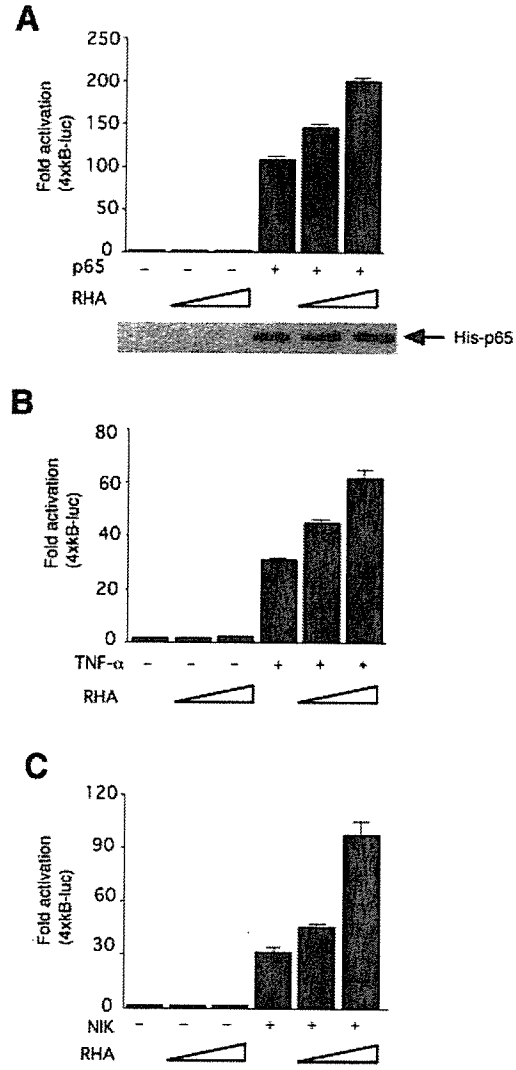

Fig. 2. RHA augments NF-κB-dependent gene expression. (A) HEK 293 cells were transfected with 20 ng of 4κB-luc in combination with pCMV-p65 [containing $(His)_6$ epitope] (10 ng) and pCMV-RHA expression plasmids (50 or 100 ng). Cells were harvested 24 h after transfection, and luciferase activity was measured. Western blot analysis of p65 levels in transfected cell extracts was done to confirm if equal amounts of the exogenous p65 are expressed irrespective of RHA overexpression (lower panel). A portion of each cell extract was separated by 10% SDS/PAGE and immunoblotted with anti-His Ig. (B) Effect of RHA on the NF-κB-dependent gene expression induced by TNF. HEK 293 cells were transfected with 4κB-luc (50 ng) and pCMV-RHA (50 or 100 ng). After 24 h of transfection, cells were stimulated with 1 ng·mL^{-1} of TNF and harvested after additional incubation for 24 h. (C) Effect of RHA on the NF-κB-dependent gene expression induced by NIK. HEK 293 cells were transfected with 4κBw-luc (50 ng) in the absence or presence of pCMV-NIK (10 ng) and pCMV-RHA (50 or 100 ng). Cells were harvested 24 h after transfection, and luciferase activity was measured. Extents of fold activation of luciferase gene expression as compared to the transfection with reporter plasmid alone are indicated. Values (fold activation) represent the mean ± SD of three independent transfections. Similar results were achieved repeatedly.

the expression plasmid for dominant negative mutant RHA, in which Lys417 of the conserved ATP-binding motif (Gly-Lys-Thr) of RHA catalytic domain was substituted by Arg, and the ATPase activity was abolished. NF-κB-dependent gene expression induced by p65, TNF-α and NIK was inhibited by the expression of RHAmATP (Fig. 3A–C), suggesting that the endogenous RHA mediates the transcriptional activity of NF-κB p65.

Effect of RHA on the p65-mediated transactivation of ICAM-1, E-selectin, and IFN-β promoters

To confirm the effect of RHA on NF-κB in physiological promoters, we examined the effect of RHA on the promoters of ICAM-1, E-selectin, and IFN-β containing NF-κB binding sites. Various amounts of RHA expressing plasmid (pCMV-RHA) or RHAmATP plasmid (pCMV-RHAmATP) were transfected into HEK 293 cells along with ICAM-1-luc, E-selectin-luc or IFN-β-luc. As shown in Fig. 4, RHA enhanced the NF-κB dependent transcription for ICAM-1, E-selectin and IFN-β promoters (Fig. 4A–C, left panels). On the other hand, overexpression of RHAmATP inhibited the NF-κB dependent transcription from ICAM-1, E-selectin and IFN-β promoters (Fig. 4A–C, right panels). These data suggest that the enzymatic activity of RHA is involved in the NF-κB mediated gene expression in physiological promoters such as IFN-β, ICAM-1 and E-selectin.

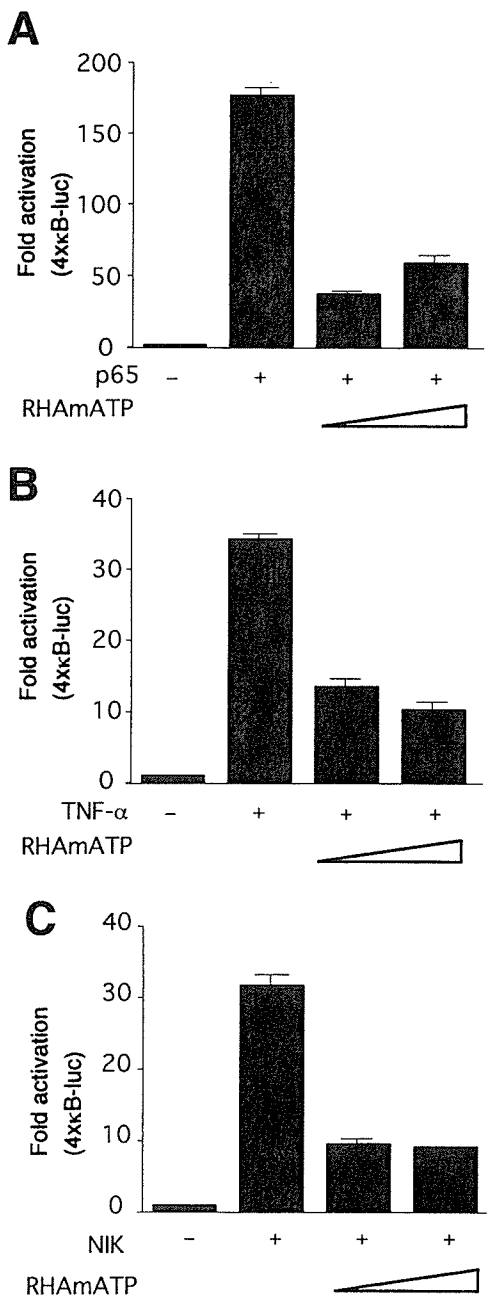

RHA activates NF-κB through activation domain of p65

To further analyze the effect of RHA on p65, we used expression plasmids for fusion proteins of Gal4-p65, Gal4-CREB or Gal4-Sp1 in which the DNA-binding domain of Gal4 was fused with p65, CREB and Sp1. The extents of augmentation of transactivation of these Gal4-p65, Gal4-CREB and Gal4-Sp1 by RHA are shown in Fig. 5. RHA augmented the transactivation mediated by Gal4-p65(1–551) and Gal4-CREB, by 1.9-fold and 3.6-fold, respectively, whereas there was no significant effect on Gal4-Sp1 (Fig. 5A). The effect of RHA on the CREB-mediated transactivation was reported previously [27]. These observations indicated that the effects of RHA on transactivation appeared relatively specific for NF-κB and CREB. To further examine whether the effect of RHA depends on the transactivation domain of p65, we used plasmids expressing various portions of p65 in fusion with Gal4 DNA-binding domain including Gal4-p65(1–551), Gal4-p65(1–286) and Gal4-p65(286–551). As shown in Fig. 5B, RHA augmented the transactivation mediated by Gal4-p65(1–551) and Gal4-p65(286–551) whereas there was no significant effect

Fig. 3. RHAmATP inhibits NF-κB-mediated transcription. (A) Inhibition of p65-mediated transcription by RHA mutant (RHAmATP) containing a single amino acid substitution in the helicase domain that abolishes its ATP-binding and helicase activity. HEK 293 cells were transfected with 20 ng of 4κB-luc in combination with pCMV-p65 (10 ng) or pCMV-RHAmATP expression plasmids (50 or 100 ng). Cells were harvested 24 h after transfection, and the luciferase activity was measured. (B) RHAmATP inhibits NF-κB-dependent transcription induced by TNF-α. HEK 293 cells were transfected with 4κB-luc (50 ng) in combination with pCMV-RHAmATP (50 or 100 ng) or the empty vector. After 24 h of transfection, cells were stimulated with 1 ng·mL^{-1} of TNF and harvested after additional incubation for 24 h (C) RHAmATP inhibits NF-κB-dependent transcription induced by NIK. HEK 293 cells were transfected with 4κBw-luc (50 ng) in combination with pCMV-NIK (10 ng) and pCMV-RHAmATP (50 or 100 ng). Cells were harvested 24 h after transfection, and the luciferase activity was measured. pCMV control plasmids were included such that all transfections had equivalent amounts of expression plasmid. Total DNA was kept at 0.5 μg with pUC19 plasmid. Cells were harvested 48 h after transfection, and luciferase activity was measured. Extents of fold activation of luciferase gene expression as compared to the transfection with reporter plasmid alone are indicated. Values (fold activation) represent the mean ± SD of three independent transfections. Similar results were achieved repeatedly.

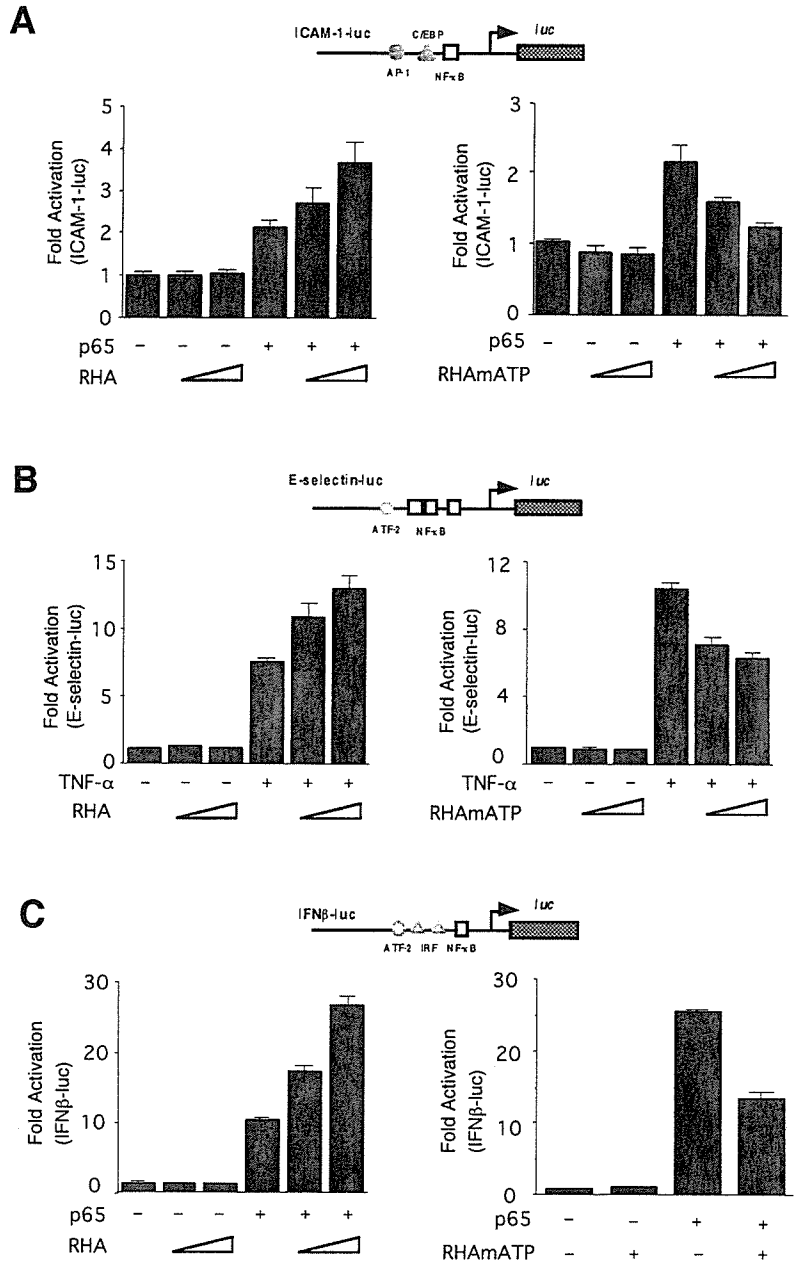

Fig. 4. RHA mediates NF-κB-dependent transcription in physiological promoters. (A) Effect of RHA on ICAM-1 promoter activity. HEK 293 cells were transfected with ICAM-1-luc (20 ng) in combination with pCMV-p65 (10 ng) and pCMV-RHA (50 or 100 ng) or pCMV-RHAmATP (50 or 100 ng). After 24 h of transfection, cells were harvested and luciferase activity was measured. (B) Effect of RHA on E-selectin promoter activity. HEK 293 cells were transfected with 20 ng of E-selectin-luc in combination with pCMV-RHA (50 or 100 ng) or pCMV-RHAmATP (50 or 100 ng). After 24 h of transfection, cells were stimulated with 1 ng·mL^{-1} of TNF-α and harvested after additional incubation for 24 h. (C) Effects of RHA on IFN-β promoter activity. HEK 293 cells were transfected with 20 ng of IFN-β-luc in combination with pCMV-p65 (10 ng) and pCMV-RHA (50 or 100 ng) or pCMV-RHAmATP (100 ng). After 24 h of transfection, cells were harvested and luciferase activity was measured. Values (fold activation) represent the mean ± SD of three independent transfections.

on Gal4-p65(1–286). These observations indicated that the C-terminal domain of p65 is required for the action of RHA.

Effect of RHA knockdown on the NF-κB-mediated transactivation

Finally, we investigated the physiological role of endogenous RHA with the use of RNA interference. We synthesized RNA duplex directed against the RHA-coding sequence (the nucleotide portion from 2408 to 2426). Transfection of HEK 293 cells with the RHA specific siRNA reduced the endogenous RHA protein level. The control siRNA had no effect (Fig. 6A). Neither RHA siRNA nor control siRNA had any effect on p65 and α-tubulin protein levels. We then examined the effect of RHA depletion on the NF-κB dependent reporter gene expression. As shown in Fig. 6B, the RHA siRNA reduced the NF-κB dependent gene expression from 4κB-luc induced by TNF-α. Similarly, we examined the effect of RHA siRNA on the TNF-mediated activation of E-selectin promoter. As shown in Fig. 6C, RHA siRNA significantly reduced the TNF-mediated induction of E-selectin gene expression. These data indicate that endogenous RHA is involved in the NF-κB-mediated gene expression.

Discussion

In this study we found that the NF-κB p65 subunit interacts with RHA *in vitro* and *in vivo*. Transient transfection assays revealed that RHA is positively involved in the

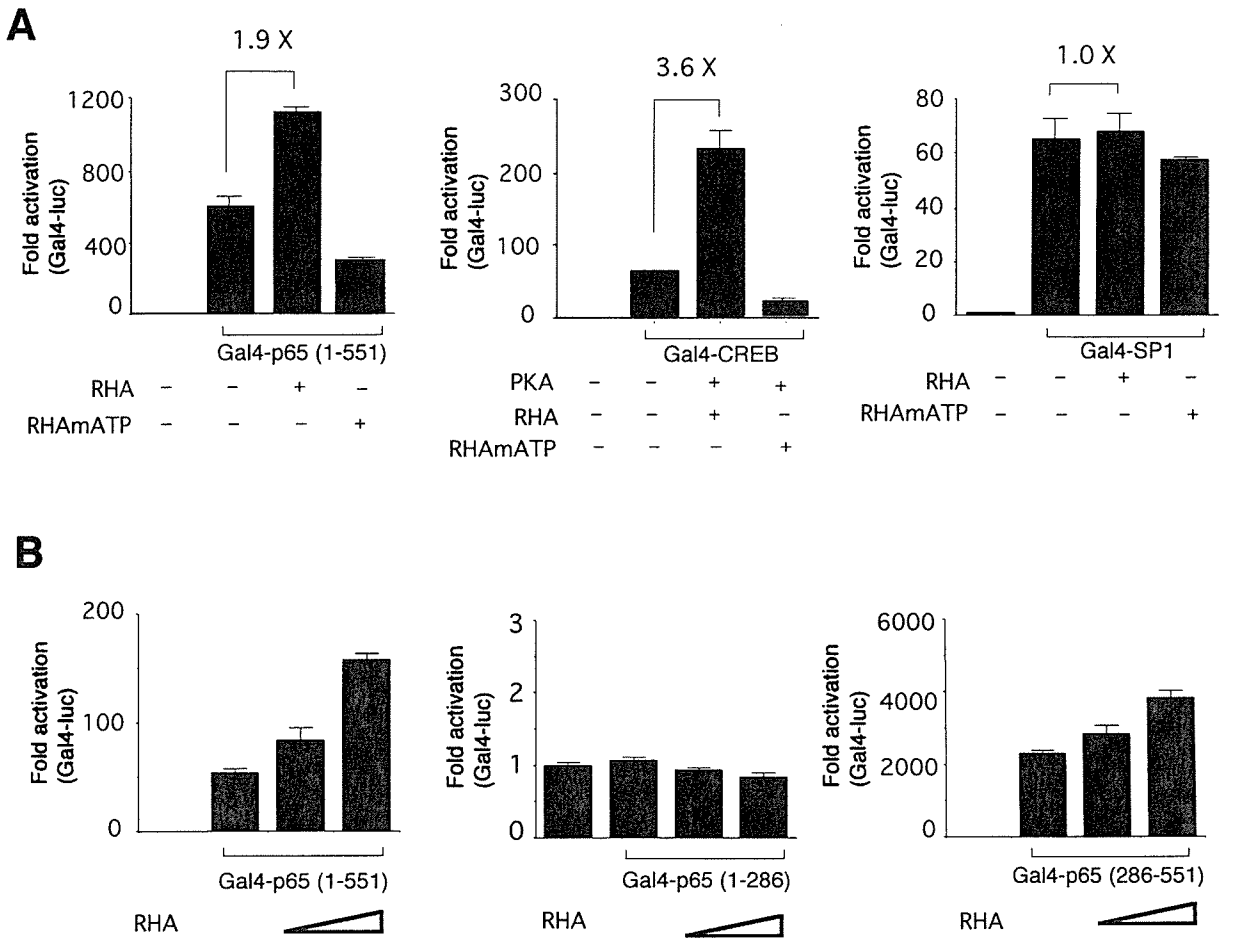

Fig. 5. Effects of RHA on Gal4-p65, Gal4-CREB and Gal4-Sp1-mediated transcription. (A) HEK 293 cells were transfected with 50 ng of 5x Gal4-luc reporter plasmid together with 10 ng of Gal4-p65 (left panel) or Gal4-CREB (10 ng) and PKA (10 ng) (middle panel) or Gal4-Sp1 (100 ng) (right panel) in combination with pCMV-RHA (100 ng) or pCMV-RHAmATP (100 ng). Cells were harvested 24 h after transfection and the luciferase activity was measured. Extents of fold activation of luciferase gene expression as compared to the transfection with reporter plasmid alone are indicated. (B) HEK 293 cells were transfected with 5x Gal4-luc reporter plasmid (50 ng) together with 10 ng of each of Gal4-p65 (1–551) (left panel), Gal4-p65 (1–286) (middle panel), Gal4-p65 (286–551) (right panel) and pCMV-RHA (100 or 200 ng). Cells were harvested 24 h after transfection, and luciferase activity was measured. Extents of fold activation of luciferase gene expression as compared to the transfection with reporter plasmid alone are indicated. Values (fold activation) represent the mean ± SD of three independent transfections.

NF-κB-dependent gene expression such as E-selectin, ICAM-1 and IFN-β. As NF-κB-dependent gene expression was inhibited by the dominant negative mutant form of RHA (RHAmATP) lacking the ATP-binding and helicase activity, the enzymatic activity of RHA is required for the transcriptional activation mediated by NF-κB.

RHA is a nucleic acid helicase that unwinds double-stranded DNA and RNA in ATP-dependent manner. It belongs to a large family of RNA helicases containing DEXD/H box that are known to be involved in various steps of gene expression including transcription, editing, splicing, RNA export, translation, and RNA turnover [31]. It is considered that RNA helicases prompt RNA molecules to initiate the interaction with other RNA molecules or proteins by catalyzing the folding and unfolding of these RNA molecules, just as proteins require chaperones to assist in folding and unfolding to form appropriate conformation [32,33].

RHA consists of two double-stranded RNA binding domains at the N-terminus, a helicase catalytic domain in the central part, and a Gly-rich single-stranded nucleic acid binding domain (RGG-box) at the C-terminus. Sequence analysis revealed that RHA contains seven helicase core motifs DEXD/H that are conserved among the helicase superfamily. It was shown previously that RHA stimulates transcription by interacting with CBP, BRCA1, and RNA Pol II [27,28]. Members of the ATPase/helicase family play important roles in many transcriptional processes including initiation, elongation, termination, and nuclear export [31]. For example, ATPase/helicase activity is found associated with TFIIH and chromatin remodeling complexes and plays crucial roles in transcriptional initiation and preinitiation. The ATPase/helicase activity of XPB/ERCC3 contained in TFIIH is required for promoter opening [34,35]. Similarly, the ATPase/helicase activity of SWI2/SNF2 in the chromatin remodeling complex SWI/SNF is involved

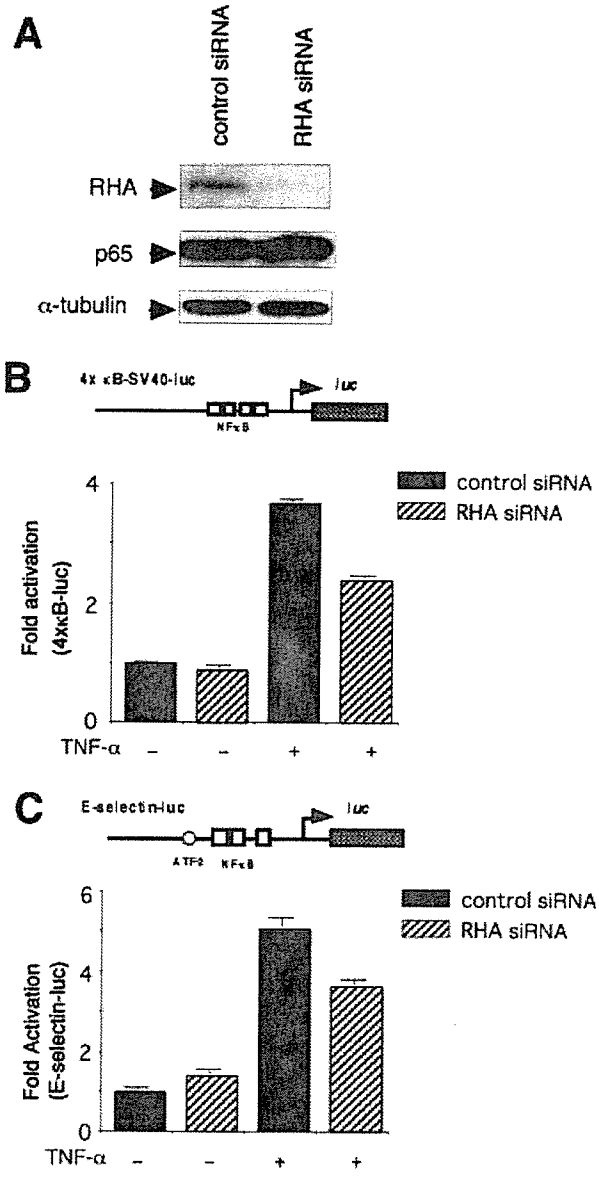

Fig. 6. Effect of RHA knockdown on NF-κB-mediated transactivation. (A) Knockdown of RHA by siRNA. HEK 293 cells (5×10^5) were transfected with 200 pmol of siRNA targeted to RHA. For the siRNA control, double-stranded RNA of unrelated sequences was used. The siRNA was transfected with lipofectamine 2000. After 48 h of transfection, cells were lysed and immunoblotted with antibodies to RHA, p65 and α-tubulin. (B) Inhibition of TNF-mediated NF-κB activation by RHA siRNA. HEK 293 cells (10^5) were transfected with 20 pmol of RHA siRNA or control siRNA together with 4κB-luc (20 ng). After 24 h of transfection, cells were stimulated with 10 ng·mL^{-1} of TNF-α and harvested after additional incubation for 24 h. (C) Inhibition of TNF-mediated E-selectin gene expression by RHA siRNA. HEK 293 cells (10^5) were transfected with 20 pmol of RHA siRNA or control siRNA together with E-selectin-luc (20 ng). After 24 h of transfection, cells were stimulated with 10 ng·mL^{-1} of TNF-α and harvested after additional incubation for 24 h. Extents of fold activation of luciferase gene expression as compared to the transfection with reporter plasmid alone are indicated. Values (fold activation) represent the means ± SD of three independent transfections. Similar results were obtained repeatedly.

in the relaxation of chromatin structure and promotes efficient transcription [36].

RHA was originally isolated as a human homologue of *Drosophila* maleless protein (MLE) [37]. MLE is involved in sex-specific gene dosage compensation and elevates the level of transcription derived from a single X-chromosome in male flies to a level equivalent to that derived from two X chromosomes in female flies [38]. MLE increases the transcriptional activity of X-linked genes through interaction with male-specific lethal (MSL) complexes [39,40]. In addition, the ATPase activity of RHA and that of MLE appeared to be essential for the CREB-dependent gene expression in mammals [27] and the gene dosage compensation in *Drosophila* [41], respectively. As MLE and its interaction with MSL are required for the specific histone H4 acetylation on X-chromosome [42,43], MLE may activate transcription of X-chromosome genes by promoting chromatin remodeling.

Another RNA helicase, p68 helicase belonging to the DEAD-box protein family, was shown to interact with human estrogen receptor α (ERα) and to act as a coactivator for ERα [44]. Although it was reported that RHA enhanced the CREB-dependent gene expression by bridging CBP and RNA Pol II, there has been no direct evidence that RHA interacts with CREB or any other gene-specific transactivators. In this study, we found that RHA binds to p65 through the interaction between the N-terminal region of RHA and the C-terminal GIR of p65. As the TA1-like and TA1 domains of p65 themselves recruit CBP/p300 coactivators, RHA appears to further facilitate the coactivator recruitment or assembly of transactivation complex by interaction with RNA Pol II.

Interestingly, we have reported previously that FUS/TLS activates the NF-κB-mediated transcription by interacting with the same region of p65 (amino acids 473–522) (GIR) [24]. There are some similarities between RHA and FUS/TLS. First, these proteins contain RGG domain that is capable of binding single-strand nucleic acids [45,46]. Second, they interact directly with the largest subunit of RNA Pol II and coactivator CBP/p300 [27,47]. Thus, NF-κB appears to form a functional transactivation complex ('enhanceosome') containing RHA, FUS/TLS, CBP/p300, RNA Pol II, and general transcription factors. Further studies are needed to clarify the action of RHA in transcriptional regulation.

Acknowledgements

We thank Drs S. T. Smale, D. Wallach, L. A. Madge, J. S. Pober, T. Nakajima, and T. Taniguchi for their generosity in providing the plasmids and RHA-antibody and Ms Angelita Sarile for language edition. We also thank Dr K. Imai and other laboratory members for critical discussions. This work was supported in part by grants-in-aid from the Ministry of Health, Labor and Welfare, the Ministry of Education, Culture, Sports, Science, and Technology of Japan and the Japanese Health Sciences Foundation.

References

1. Baldwin, A.S. Jr (1996) The NF-kappa B and I kappa B proteins: new discoveries and insights. *Annu. Rev. Immunol.* **14**, 649–683.